

We are IntechOpen, the world's leading publisher of Open Access books Built by scientists, for scientists

6,900

Open access books available

185,000

International authors and editors

200M

Downloads

Our authors are among the

154

Countries delivered to

TOP 1%

most cited scientists

12.2%

Contributors from top 500 universities



WEB OF SCIENCE™

Selection of our books indexed in the Book Citation Index
in Web of Science™ Core Collection (BKCI)

Interested in publishing with us?
Contact book.department@intechopen.com

Numbers displayed above are based on latest data collected.
For more information visit www.intechopen.com



Improvement of Oxygen Transfer Efficiency in Diffused Aeration Systems Using Liquid-Film-Forming Apparatus

Tsuyoshi Imai and Hua Zhu

*Division of Environmental Science and Engineering,
Graduate School of Science and Engineering,
Yamaguchi University
Japan*

1. Introduction

Currently, aerobic bio-treatment processes, in which activated sludge system is at the center of the attention, are extensively applied in sewage treatment plants around the world. For activated sludge process, the diffused aeration has been thought to be one of the most important and indispensable operational units. However, a major concern of this operational methodology is that a large amount of compressed air has to be consumed in a diffused aeration system owing to the low oxygen transfer efficiency in water. It has been previously demonstrated that more than 40 % of the total power consumption in sewage treatment plants in Japan is related to power consumption associated with aeration alone. Therefore, the development of highly efficient aeration strategies has presently emerged as an intriguing research topic in the field of energy savings.

The oxygen transfer in diffused aeration systems can be divided into two processes: bubble oxygen transfer and surface oxygen transfer. Bubble oxygen transfers into the water across the bubble-water interface as the bubbles rise from the diffuser to the water surface. Surface oxygen transfer exclusively occurs at the air-water interface situating on the water surface, originating from vigorous turbulence induced by bubble-plume motion and water circulation. Wilhelms and Martin's findings indicated that approximately one-third of the total volumetric mass transfer coefficient (k_{La_t}) is responsible for the volumetric mass transfer coefficient for surface transfer (k_{La_s}) [1]. McWhirter and Hutter determined that a representative k_{La_s} is 25-33 % of the k_{La_t} in a fine bubble diffuser system and 11-17 % of the k_{La_t} in a coarse bubble diffuser system [2]. DeMoyer *et al.* ever reported that the k_{La_s} is 59-85 % of the volumetric mass transfer coefficient for bubble surface (k_{La_b}) [3].

Bubble transfer and surface transfer both contribute remarkably to the total oxygen transfer in the submerged aeration system. However, bubble transfer is the predominant means of oxygen transfer. So far, considerable research interests have been focused on the enhancement of the bubble transfer efficiency by developing a wide variety of new aeration techniques, including the utilization of high-purity-oxygen aeration system [4-10], deep aeration system [11-13] and fine bubble diffuser [14-17], *etc.* Nevertheless, only a little effort has been devoted to the research on the improvement of surface transfer efficiency.

The improvement of oxygen transfer capability across water surface is pursued in this study. The objective is fulfilled with a liquid-film-forming apparatus (LFFA) by pre-forming an aggregative entity in the atmosphere near water surface. This entity is constructed of a large quantity of air-filled gas bubbles with the periphery of each gas bubble surrounded by an ultrathin layer of liquid film, thereby enlarging notably the effective interfacial contact area between air and water. Consequently, energy consumption problem can be solved by reducing the aeration depth down to 1 m or less without trading off the ideal aeration efficacy in a diffused aeration system. Based on the concept above, lab-scale experimental apparatus is designed in this study and the efficiency of oxygen transfer in this novel apparatus is determined either numerically or experimentally. Furthermore, a number of factors affecting the efficiency of oxygen transfer are also examined in detail, and the feasibility is preliminarily explored for the application in wastewater treatment plants.

2. Novel idea: Liquid-film aeration system (LFAS)

Liquid-film aeration system (LFAS) which means that LFFA developed in this study is installed on the water surface of existing aeration tanks. Under no extra energy consumption circumstances, water body is wholly membranized into a liquid film (i.e., a thin water film located at the water surface-air interface) by LFFA, thus realizing the oxygen supply towards liquid-film-formed water body simultaneously from the interior and exterior of the liquid film. The efficiency of atmospheric oxygen enrichment is improved as a consequence of dual-fold oxygen provisions. Namely, in addition to the existing oxygen supply efficiency of an aeration tank, the oxygen supply efficiency of LFAS is increased by one more term from the LFFA. As a result, the oxygen supply efficiency of the entire aeration system is enhanced.

Schematic drawings of the LFFA are illustrated in Fig. 1. The LFFA, made of plastics here, has a simple configuration constituting three sections: (1) trumpet-shaped capture part as a gas collector for converging the released gas bubbles; (2) airlift part, mainly made up of some pipes orienting parallel to each other, aiming to facilitate the relevant liquid film formation near the water surface and (3) effluent part which alternately reserves and discharges the treated water involving higher-concentration dissolved oxygen (DO).

Optionally, the LFFA can be compatibly installed in an existing aeration system. The whole set of equipment is denoted as liquid-film aeration system (Fig. 2). The joint interface between the capture and airlift parts of this LFFA is flush with the water surface with the former just submerged in water and the latter completely exposed to air. During the operating process, the gas bubbles released from a diffuser first rise to the airlift part through the capture part and then self-assemble into a macroscopic aggregated system of gas bubbles over the airlift part. This macroscopic ensemble of gas bubbles floating in the atmosphere in close proximity to the water surface are microscopically comprised of the combination of numerous agglomerated gas bubbles and a fraction of the bulk water (serving as liquid-film boundary layer surrounding each individual bubble herein) entrained by the ascending bubbles. In this case, air fills both the exterior and interior of these bubbles as well as the thin liquid film, as described above. Hence, oxygen transfer can take place both across the inner interface (gas bubble and liquid film) and the outer interface (atmosphere and liquid film) of the thin liquid film, which means that the available interfacial contact area between oxygen and water can be greatly multiplied, thereby promoting effectively oxygen transfer efficiency. Subsequently, oxygenic water is

discharged downstream from the effluent part. Furthermore, LFAS can supply oxygen either in a once-through mode in the case of which the effluent part is directly connected to another water reservoir, or in a recycle mode in the case of which the effluent part is directly connected to the original water tank itself.

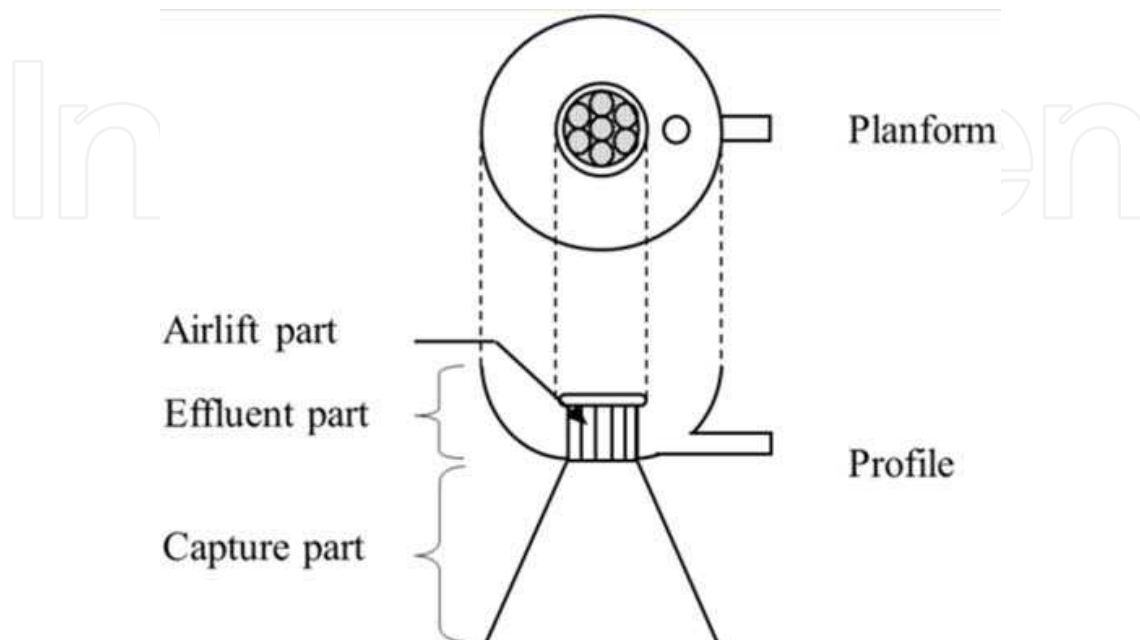


Fig. 1. Schematic diagram of the LFFA

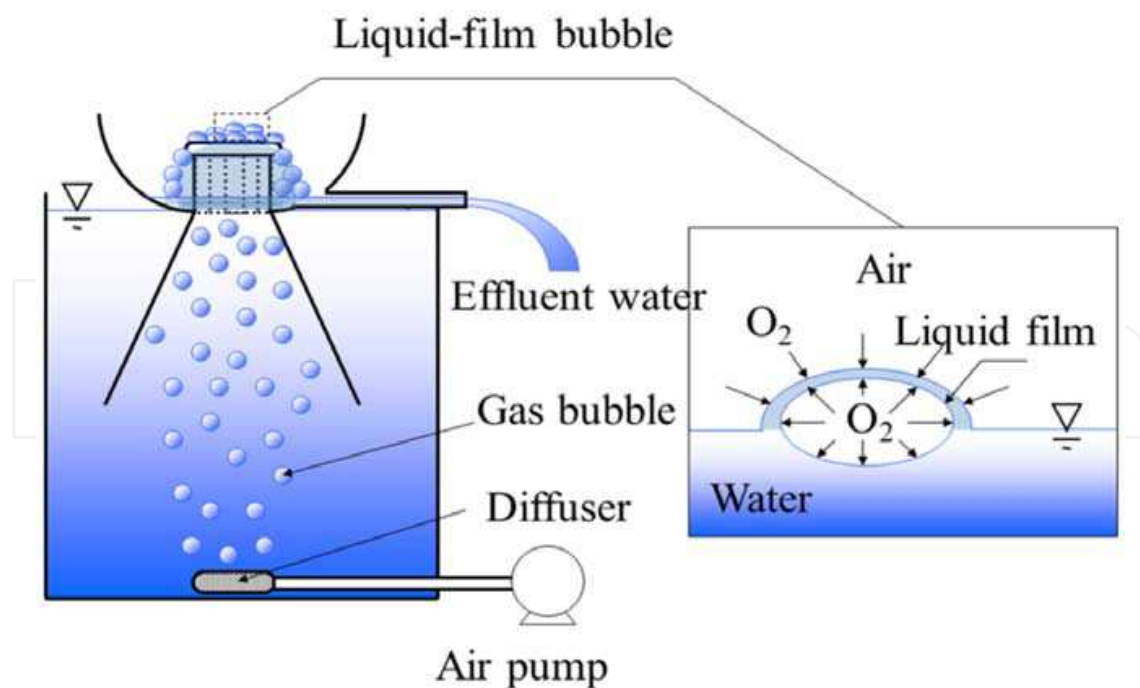


Fig. 2. Liquid-film aeration system (LFAS)

The picture of the actual experimental apparatus is shown in Fig. 3. Fig. 4 reveals the form of a liquid film.



Fig. 3. Lab-scale LFFA



Fig. 4. The picture of forming liquid film

LFAS possesses the following characteristics.

Due to the superior oxygen supply efficiency, even if the aeration depth is as low as less than 1 m, a sufficient amount of oxygen can still be provided. In contrast, the conventional aeration tank necessitates a depth of 4-5 m to achieve a commensurate oxygen supply. Therefore, LFAS is a very energy-saving aeration system.

Although some energy is consumed as a consequence of the friction between the airlift tube wall of LFFA and surrounding water body, we suggest that this portion of energy consumption is far below the wasted energy in the conventional aeration system. Moreover, the energy wasted in the traditional aeration system can be re-used for the oxygen supply. Therefore, this novel LFAS-based method definitely opens an energy-efficient pathway to improve the oxygen transfer efficiency.

LFFA has a very simple structure, and its production cost is very low. Optionally, it can be made from recycled plastics. As another advantage, this apparatus itself does not consume any power, and can be easily installed on the water surface of existing aeration tank without large-scale retrofitting. Thus this very cheap setup is well suited for the application in the recycle-type society.

3. Pre-experiment on the LFFA

3.1 Introduction

In order to evaluate the oxygen transfer performance of the LFFA, under the experimental conditions of different bubble diameters and different aeration amounts, comparative experiments are conducted on a liquid-film aeration system and conventional aeration system by respectively using de-oxygenated water and activated sludge.

3.2 Experimental methods

The diffuser is set in a 28.5 cm deep and 15 L capacity cylindrical water tank with a surface area of 526.3 cm². Its location is at the middle of the experimental water tank bottom with an aeration depth of 26 cm. The liquid-film apparatus with a pipe diameter of 1 cm, effective height of 10 cm and cross-sectional area of 12.56 cm² is mounted on the surface of a water tank. During the operational period, single-pass fashion is employed for this apparatus. After measurement of DO concentration and temperature in the initially de-oxygenated water, a given amount of aeration is provided and the aeration lasts for 4 min. The DO concentration in the discharged water from the effluent part is periodically measured at a sampling interval of 30 s. The amount of the effluent water is calculated before the aeration is suspended. To prevent the water surface in the water tank from going downwards, the volume of the de-oxygenated water equivalents to that of the treated water is periodically poured into the water tank to maintain the water surface's balance throughout the experiment. As a control, the conventional aeration experiment is also conducted at the same water disposal volume, aeration depth and aeration duration as the liquid-film aeration experiment. The experimental setup is demonstrated in Fig. 5.

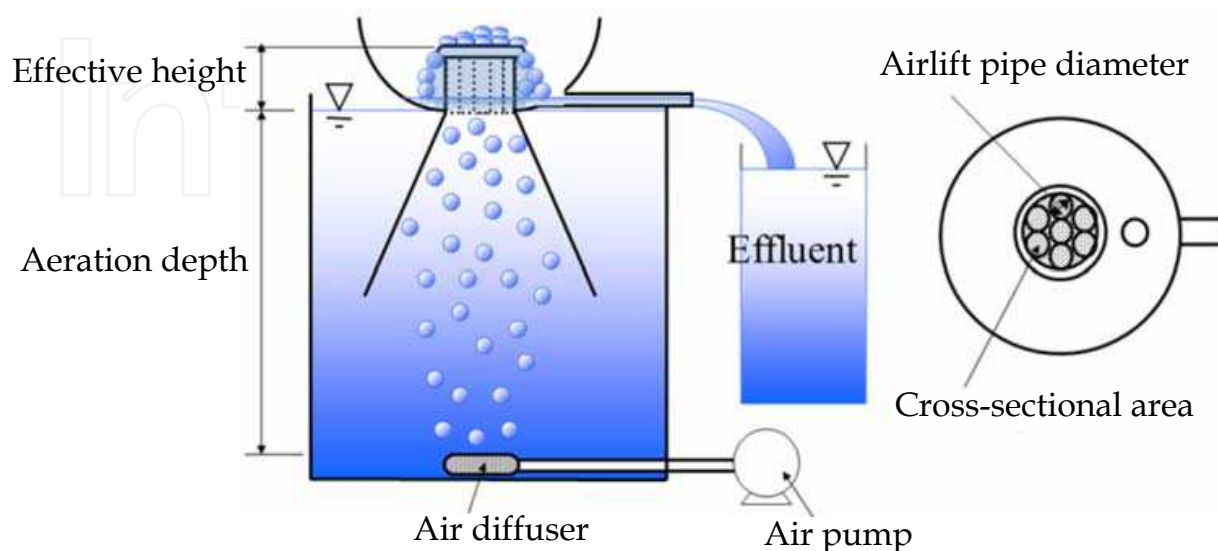


Fig. 5. Single-pass LFFA apparatus

A 0.08 g/L sodium sulfite solution is used to chemically de-oxygenate the tank water to around 0 mg/L at the start of each test. The activated sludge is taken from Ube Eastern Water Cleanup Center. DO concentrations are determined by YSI Model DO meter. Two types of air pumps (Iwaki APN-215CV-1 Model and Secoh DF-406 Model) are used herein. Two kinds of air diffusers are selected providing average gas bubble diameters of 3 and 6 mm, respectively. A series of the combinations of diffuser and air pump give rise to different aeration amounts, as shown in Table 1. The average bubble diameter is determined by averaging the diameters of several digital-camera-taken gas bubbles just released from the diffuser.

Average bubble diameter of a diffuser	Air pump type	Air flow rate
3 mm	APN-215CV-1	12.8 L/min
3 mm	DF-406	18.6 L/min
6 mm	APN-215CV-1	13.5 L/min
6 mm	DF-406	19.2 L/min

* Adjusting aeration amounts contingent on different experimental conditions.

Table 1. The air flow rate as a function of diffuser and air pump types*

The experimental results are compared in terms of DO saturation rate and oxygen transfer rate, both of which are calculated by the following Equations (1) and (2),

$$\text{DO saturation rate (\%)} = \frac{DO_{act}}{DO_{sat}} \times 100\% \quad (1)$$

$$\text{Oxygen mass transfer rate (mg-O}_2\text{/min)} = (DO_{act} - DO_0) \times Q_L \quad (2)$$

where DO_{act} is the measured DO average value in mg/L, DO_{sat} is the saturated DO concentration in water at 1 atm in mg/L, DO_0 is the initial DO concentration in mg/L, and Q_L is the flow rate of the effluent water in L/min.

3.3 Results and discussion

3.3.1 DO saturation rate

Fig. 6 and Fig. 7 respectively show the experimental data using de-oxygenated water and DO saturation rate using activated sludge.

As shown in Figs. 6 and 7, independently of air flow rate and aerated bubble diameter, it is suggested from both de-oxygenated water and activated sludge experiments that the effluent DO concentration associated with liquid-film aeration is always higher than that by conventional aeration. While de-oxygenated water is in service, conventional aeration yields a DO saturation rate of 80%, in contrast to up to ca. 95% by way of liquid-film aeration. Even in the case of activated sludge, the corresponding value of over 90% is achieved via liquid-film aeration. It is found that in comparison with the conventional aeration by using continuously recirculated aeration to enhance DO concentration, for the liquid-film aeration, the DO content in the effluent can be raised up to the saturation state by only aerating once the effluent, thereby indicating strong oxygen supply capability of the latter.

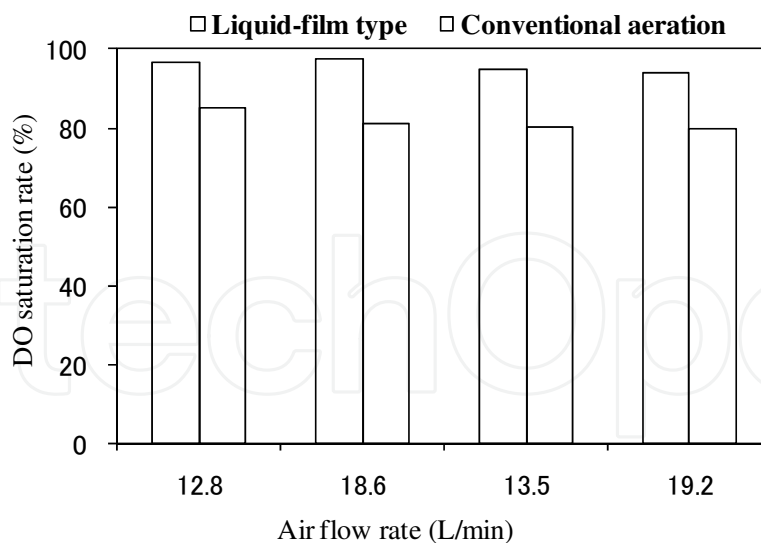


Fig. 6. The comparison of DO saturation rate (de-oxygenated water)

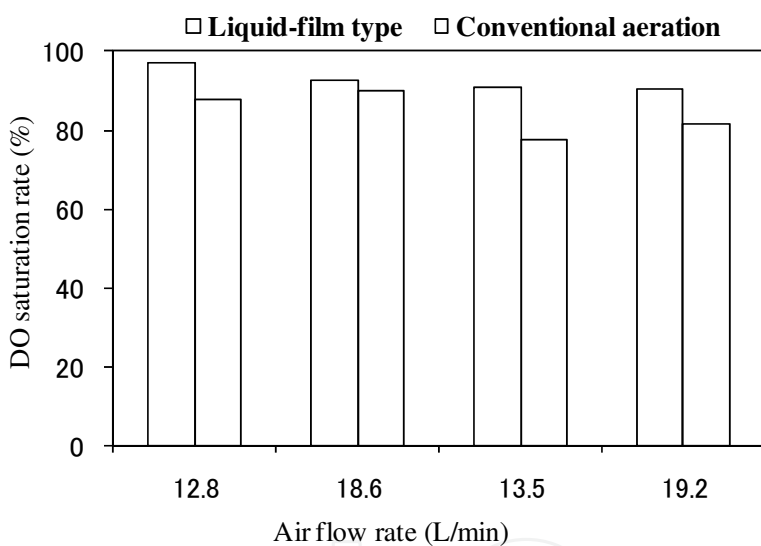


Fig. 7. The comparison of DO saturation rate (activated sludge)

3.3.2 Oxygen mass transfer rate

Figs. 8 and 9 show the oxygen mass transfer rates for the de-oxygenated water and activated sludge, respectively. As shown in these experimental findings, whether for de-oxygenated water or activated sludge, the smaller the gas bubble diameter or the higher the aeration amount at the same gas bubble diameter is, the faster the oxygen transfer rate is. While the de-oxygenated water is in use, oxygen transfer rate of liquid-film aeration increases by 30% in regard to conventional aeration. In the case of activated sludge, an increase of 10% is correspondingly observed.

As indicated in Figs. 8 and 9, liquid-film apparatus only needs an aeration depth of a few tens of centimeters to provide adequate amount of oxygen. However, 4-5 m in aeration depth is required for the conventional aeration apparatus to supply comparable oxygen content. Hence, liquid-film apparatus is regarded as a very energy-efficient setup.

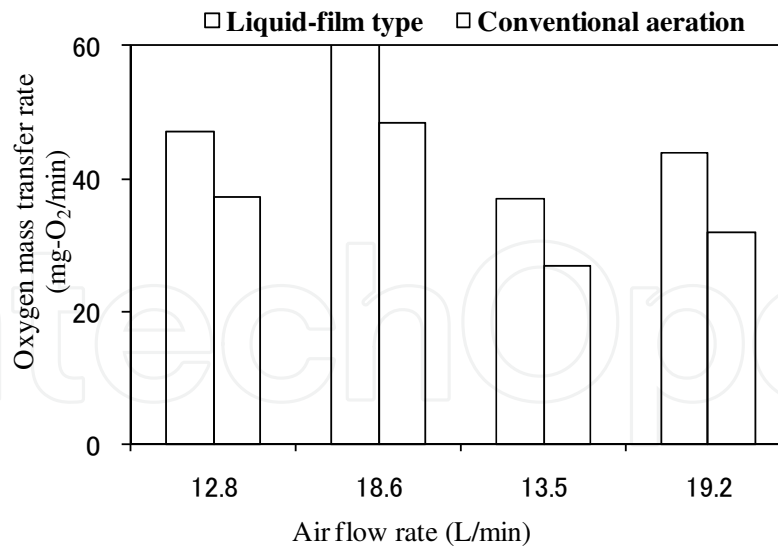


Fig. 8. The comparison of oxygen mass transfer rate (de-oxygenated water)

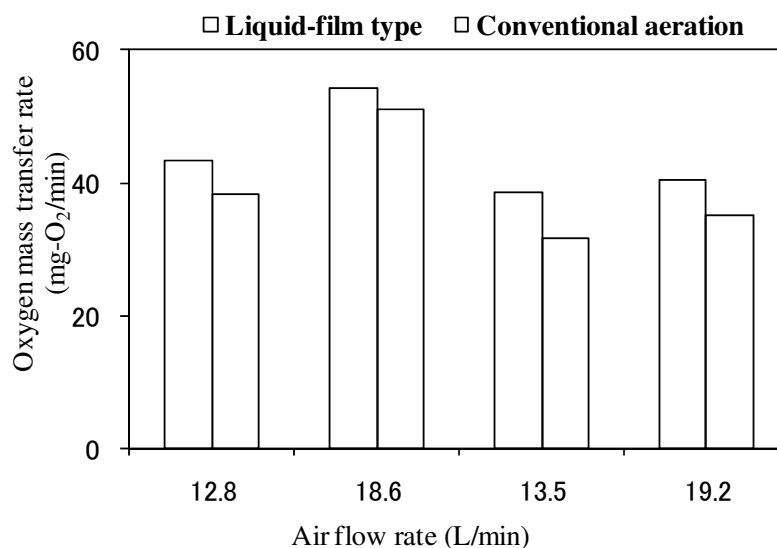


Fig. 9. The comparison of oxygen mass transfer rate (activated sludge)

4. Effect of the structural parameters of the LFFA

4.1 Introduction

According to the preceding pre-experiment on the LFFA, the basic factors influencing liquid film formation involve airlift pipe diameter, cross-sectional area, effective height, air flow rate, gas bubble diameter and aeration depth, etc. This section will discuss experimentally the effect of every factor on liquid film formation in detail, and the optimal design parameter of LFFA will then be identified.

Fig. 10 demonstrates a variety of factors impacting the liquid film formation. Each factor is defined as follows. Effective height refers to the length of airlift, and +/- symbols represent the lengths above/below the water surface, respectively. Aeration depth represents the distance from the diffuser to water surface, and cross-sectional area means the cross-sectional area of the airlift part.

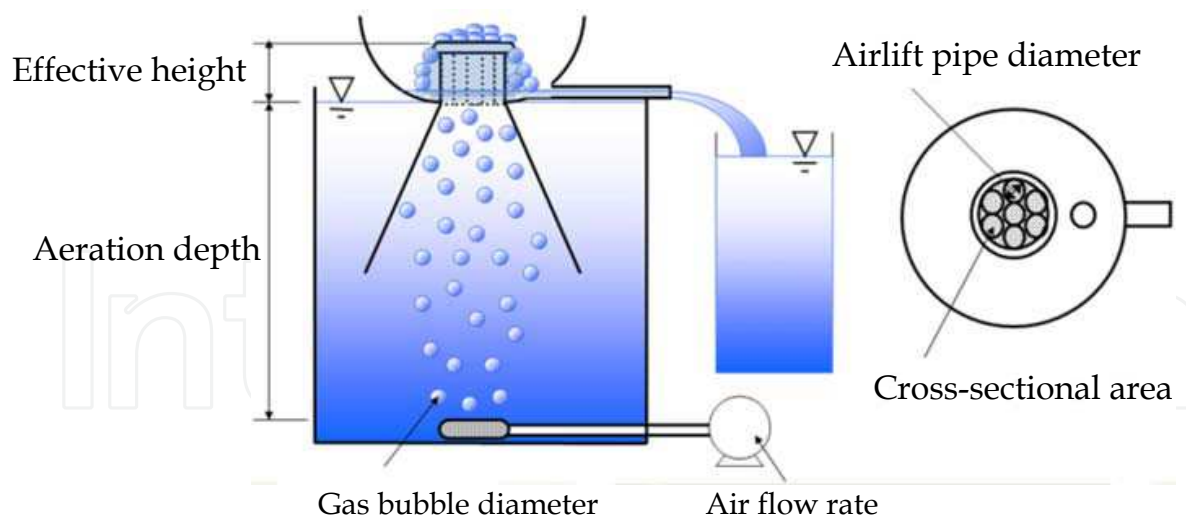


Fig. 10. The factors affecting the liquid film formation

4.2 Effect of altering gas bubble diameter on oxygen supply efficiency

4.2.1 Experimental conditions

In this trial, gas bubble diameter is varied by changing the type of diffuser. Diffuser can offer 2 kinds of gas bubbles with a diameter of 3 and 6 mm, respectively. The various combinations of diffuser and air pump as well as air flow rate are listed in Table 1. The average gas bubble diameter is determined by averaging the diameters of many digital-camera-taken gas bubbles located near the diffuser.

The parameter of the single-pass LFFA apparatus is listed as follows: 4, 6 and 10 mm in pipe diameter, 10 cm in effective height, and 12.56 cm² in cross-sectional area. The rig of experimental apparatus and experimental conditions are respectively shown in Fig. 11 and Table 1.

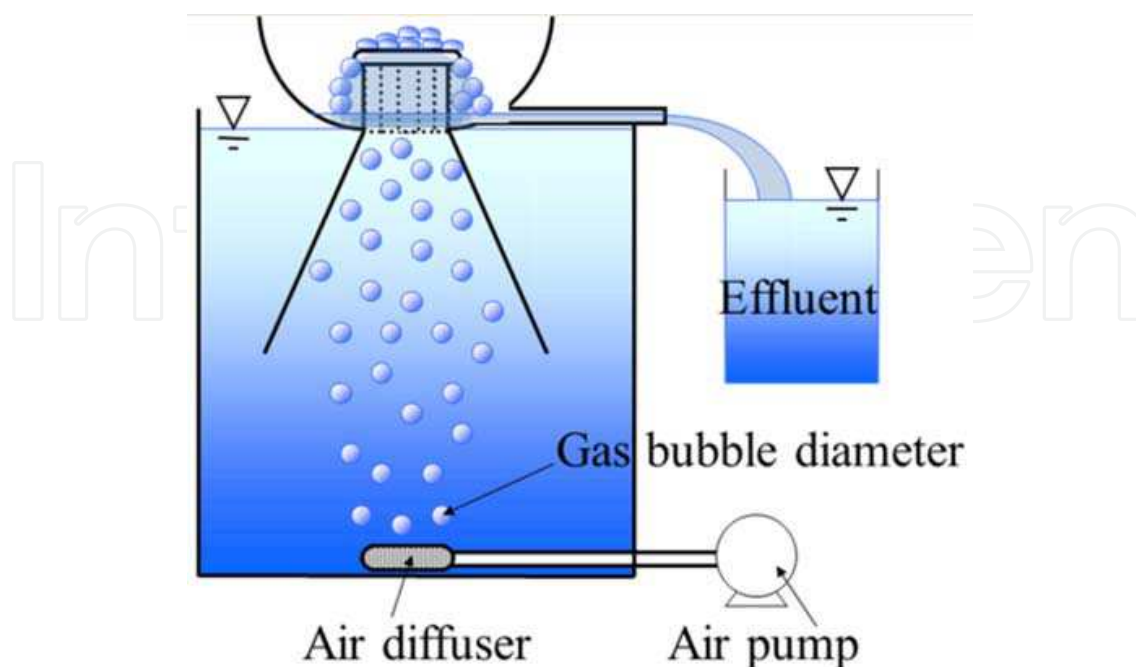


Fig. 11. Experimental apparatus relating to the variation in gas bubble diameter

4.2.2 Experimental methods

The LFFA operating in a single-pass manner is set in a 28.5 cm deep and 15 L cylindrical tank with a surface area of 526.3 cm². After measurement of DO concentration and temperature in the initially deoxygenated water, a given amount of aeration is provided and lasts for 4 min. The DO concentration in the discharged water from the effluent part is periodically measured at an interval of 30 s. The amount of the effluent water is calculated before aeration is stopped. To prevent the water surface in the water tank from going downwards, the volume of the de-oxygenated water equivalent to that of the treated water is periodically poured into the water tank to maintain the water surface's balance throughout the experiment.

DO concentrations are determined with YSI Model DO meter. Air pump includes Iwaki APN-215CV-1 Model and Secoh DF-406 Model.

4.2.3 Calculation methods

The parameters such as DO saturation rate, oxygen transfer rate and oxygen transfer mass per unit air aeration volume are used for evaluating the experimental results in this experiment. The calculation is based on Equations (1), (2) and (3).

$$E_O = \frac{(DO_{act} - DO_0) \times Q_L}{Q_G} \quad (3)$$

Herein, E_O stands for oxygen transfer mass per unit air aeration volume in mg-O₂/L-air, DO_{act} is the actually measured average DO concentration in mg/L, DO_0 is the initial DO concentration in mg/L, Q_L is the effluent flow rate in L/min, Q_G is air flow rate in L/min.

4.2.4 Results and discussion

The experimental results of the DO saturation rate, effluent flow rate, oxygen mass transfer rate and oxygen transfer mass per unit air aeration volume are respectively shown in Figs. 12, 13, 14 and 15.

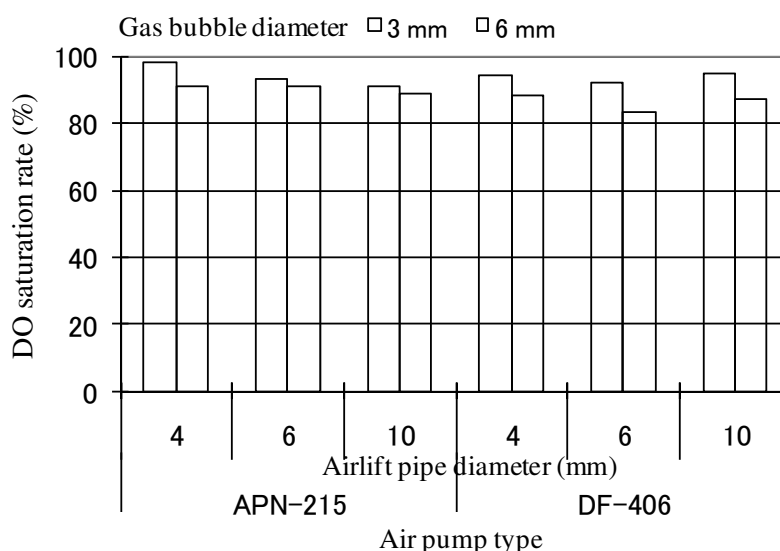


Fig. 12. Effect of gas bubble diameter on the DO saturation rate

As indicated in Fig. 12, DO saturation rates always maintain higher than 80% in all experiments, suggesting the superior oxygen transport ability of this novel setup. In Fig. 12, when the same air pump is used, the aeration amount of the diffuser providing a gas bubble diameter of 3 mm is less than that of the diffuser with a bubble diameter of 6 mm. However, it is found from the experiment results of 4 mm pipe diameter that though the aeration amount is comparatively small for the 3 mm diameter bubbles, DO saturation rate is still higher than that of 6 mm diameter bubbles. Likewise, the same trend is observed for the 6 and 10 mm diameter pipes. This is attributed to the fact that the finely divided gas bubbles allow for the enlarged contact area between water and gas bubbles in the aeration system, thereby enhancing the oxygen transport ability.

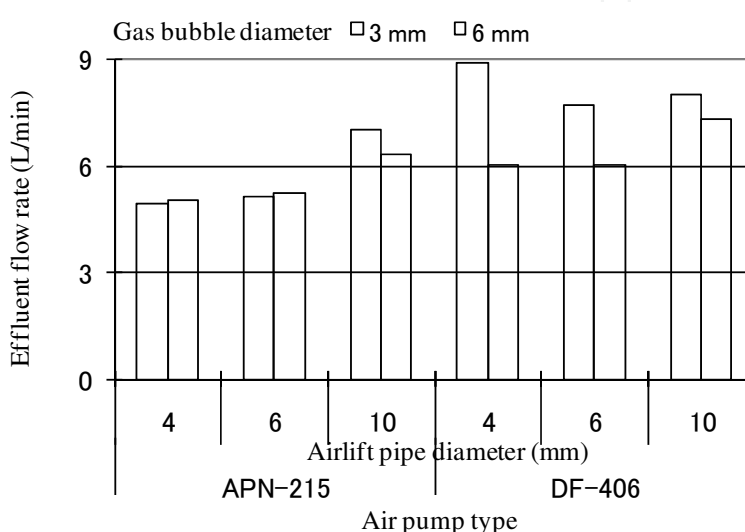


Fig. 13. Effect of gas bubble diameter on the effluent flow rate

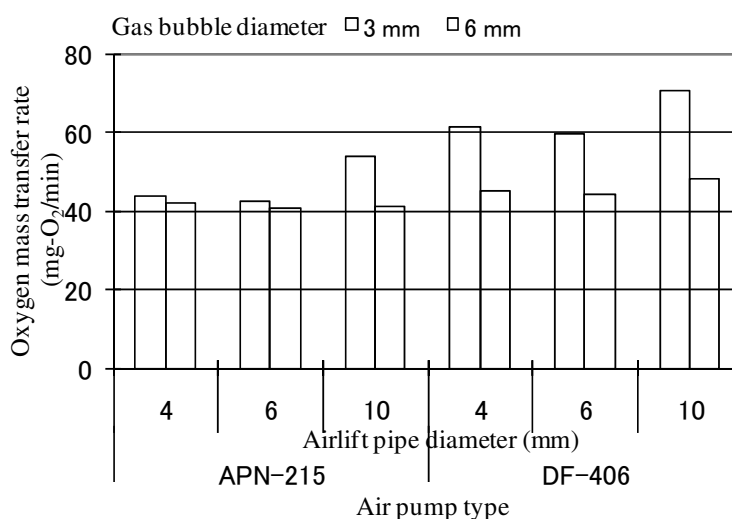


Fig. 14. Effect of gas bubble diameter on oxygen mass transfer rate

As shown in Figs. 13 and 14, both effluent flow rate and oxygen transfer rate exhibit a tendency same as DO saturation rate. However, as a result of the different aeration amounts applied, it is very hard to make a credible judgement.

Therefore, the parameter E_0 (DO amount per unit oxygen supply amount) is introduced herein. Its experimental result is shown in Fig. 15. As shown in this figure, when the pipe diameters are 4, 6 and 10 mm, the same trends are all manifested. That is, E_0 of 3 mm diameter gas bubble is greater than that of 6 mm.

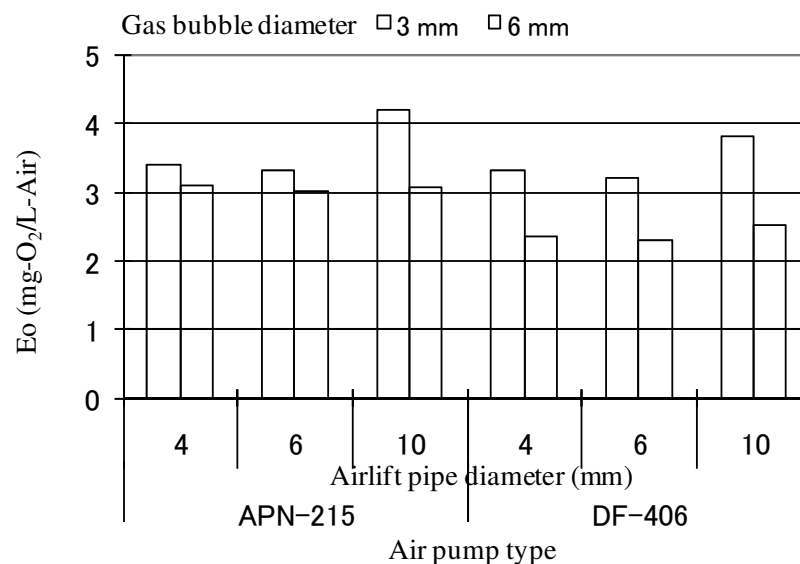


Fig. 15. Effect of gas bubble diameter on E_0

Similarly, while the other air pump is used, the similar evolving trends are observed for DO saturation rate, effluent flow rate, oxygen transfer rate and oxygen transfer efficiency. Namely, the smaller the gas bubble diameter is, the higher the result is. It is shown that the LFFA is likewise subjected to the effect of the interfacial contact area between air and water.

4.3 Effect of aeration depth on oxygen supply efficiency

4.3.1 Experimental conditions and methods

At an air flow rate of 13.5 L/min, aeration depth is respectively set at 26 and 63 cm. LFFA adopts a single-pass apparatus with a pipe diameter of 6 mm, effective height of 10 cm and cross-sectional area of 12.56 cm². The diffuser in connection with an Iwaki APN-215CV-1 Model air pump can release gas bubbles with an average diameter of 3 mm. The experimental apparatus relating to the differing aeration depths is shown in Fig. 16.

Experimental methods refer to Section 4.2.2.

The experimental results are evaluated in terms of DO saturation rate (*cf.* Equation 1) and oxygen transfer rate (*cf.* Equation 2).

4.3.2 Results and discussion

The experimental results are shown in Table 2. The larger the aeration depth is, the higher the DO saturation rate, effluent flow rate and oxygen transfer rate are. Thus, the oxygen supply ability of LFFA also obeys the oxygen diffusion regime at the gas-liquid interface.

At an aeration depth of 63 cm, the DO concentration in the effluent stream approximately approaches the saturation value, thereby determining the feasible aeration depth located at roughly 60 cm for the LFAS.

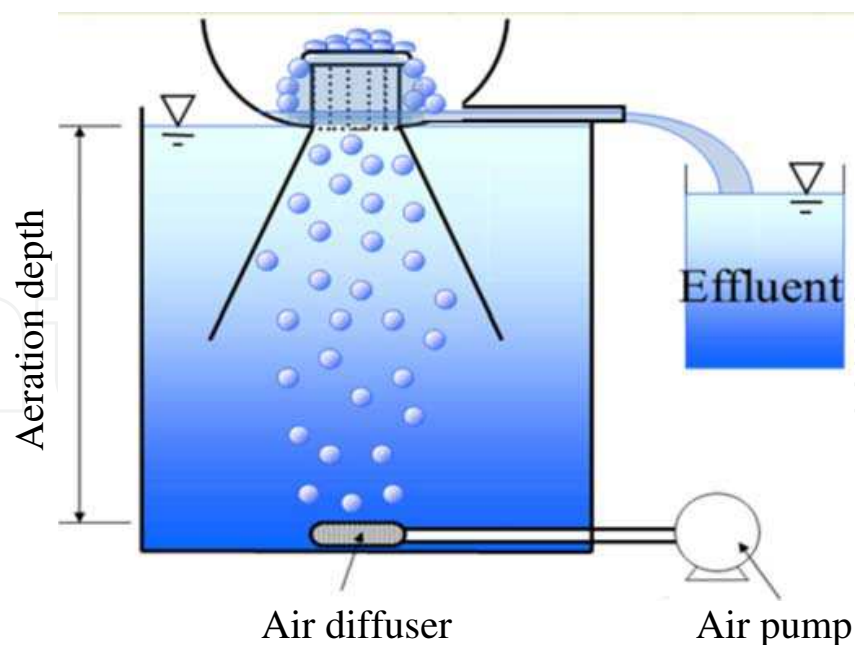


Fig. 16. Experimental apparatus relevant to the change in aeration depth

Aeration depth (cm)	Effluent flow rate (L/min)	DO saturation rate (%)	Oxygen mass transfer rate (mg-O ₂ /min)
26	5.36	83.7	37.4
63	5.60	98.5	44.1

Table 2. Experimental results pertaining to the variation in aeration depth

4.4 Effect of pipe diameter on oxygen transfer efficiency

4.4.1 Experimental conditions and methods

Three series of experiments are carried out with pipe diameters of 0.6, 1, 2, 4 and 5 cm, and effective heights of 1, 5 and 10 cm. At the pipe diameter of 0.6, 1, 2 and 4 cm, the diameter of the airlift part is set at 4 cm to attain the same cross-sectional area. By contrast, at a pipe diameter of 5 cm, setting the airlift part diameter at 5 cm leads to the altered cross-sectional area. In order to maintain the same aeration flux, the air flow rate is correspondingly increased when conducting this series of experiments involving 5 cm diameter pipes.

Experimental conditions and experimental apparatus diagram are respectively shown in Table 3 and Fig. 17.

Pipe diameter (cm)	Air flow rate (L/min)	Cross-sectional area (cm ²)	Aeration flux* [L/(min · cm ²)]	Effective height (cm)
0.6, 1, 2, 4	12.8	12.5	1.0	1, 5, 10
5	20.0	19.6	1.0	

* aeration flux : air flow rate per unit cross-sectional area.

Table 3. Experimental conditions relating to various pipe diameters

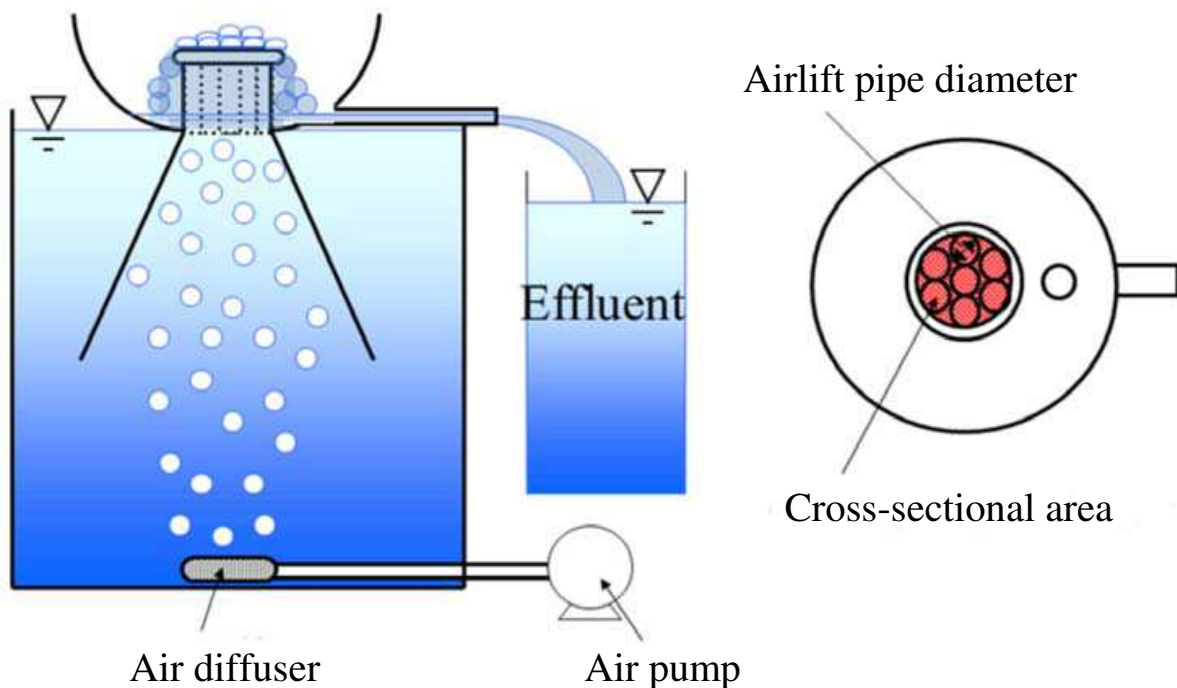


Fig. 17. Experimental apparatus relevant to various pipe diameters

The evaluation criteria include DO saturation rate (*cf.* Equation 1), liquid/gas ratio and E_0 (*cf.* Equation 3). The calculation of liquid/gas ratio is given by Equation 4.

$$\text{Liquid/gas ratio} = Q_L/Q_G \quad (4)$$

where Q_L refers to the effluent flow rate (L/min) and Q_G is air flow rate (L/min).

4.4.2 Results and discussion

The effect of pipe diameter on DO saturation rate, liquid/gas ratio, and E_0 is shown in Fig. 18.

Irrespective of effective height, DO saturation rate, liquid/gas ratio and E_0 all exhibit similar trends. DO saturation rate tends to become large with decreasing pipe diameter. This is due to the fact that when the gas bubbles are passing through the LFFA setup, they are finely split, thereby enlarging dramatically the surface area of liquid film and consequently accelerating oxygen transport speed.

Liquid/gas ratio slowly increases with increasing pipe diameter and reaches the maximum value at 4 cm in pipe diameter. Because finely splitting of gas bubbles in the airlift part consumes some energy, the larger the pipe diameter, the smaller the hydraulic head loss in the airlift part, which thus increases the water flow rate there. However, if pipe diameter is over-sized, the airlift effect will be weakened, resulting in the reduced water flow rate through the airlift part. A direct outcome of interacting the 2 factors above with each other is the occurrence of an optimal parameter under a certain condition.

As shown by Equation 3, both DO concentration and liquid/gas ratio in the effluent water have an effect on oxygen transfer amount per unit air aeration volume, and 3 optimal conditions arise. They are listed as follows: (1) 4 cm in pipe diameter and 1 cm in effective height; (2) 4 cm in pipe diameter and 5 cm in effective height, and (3) 0.6 in pipe diameter

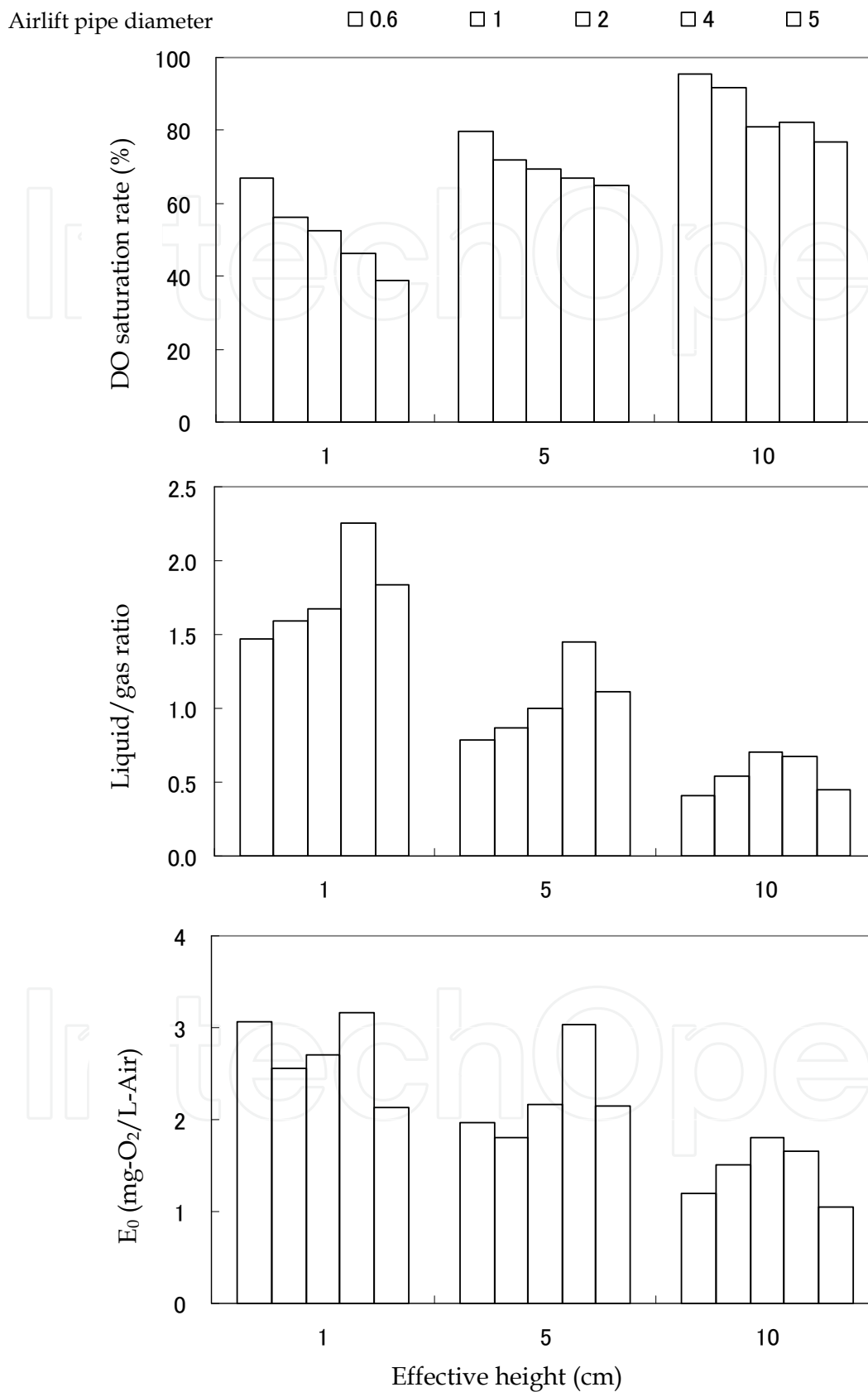


Fig. 18. Effect of airlift pipe diameter

and 1 cm in effective height. Meanwhile, as shown in Fig. 18, under the first condition, DO concentration relatively significantly affects oxygen transfer amount per unit air aeration volume. In contrast, liquid/gas ratio in the effluent plays a comparatively pronounced role under the third condition.

4.5 Effect of effective height on oxygen supply efficiency

4.5.1 Experimental conditions and methods

Effective height stands for airlift height. In this trial, the effective height is set at 1, 5 and 10 cm. Herein, the other structural parameters of the single-pass LFFA are 1, 2 and 4 cm in pipe diameter and 12.56 cm² in cross-sectional area. Air flow rate is 12.8 L/min.

Experimental conditions and experimental data are shown in Table 4 and Fig. 19, respectively.

DO saturation rate, liquid/gas ratio (*cf.* Equation 4) and E_0 (*cf.* Equation 3) are used as the evaluation criteria.

Effective height (cm)	Pipe diameter (cm)	Air flow rate (L/min)
1, 5, 10	1, 2, 4	12.8

Table 4. Experimental conditions linked to various effective heights

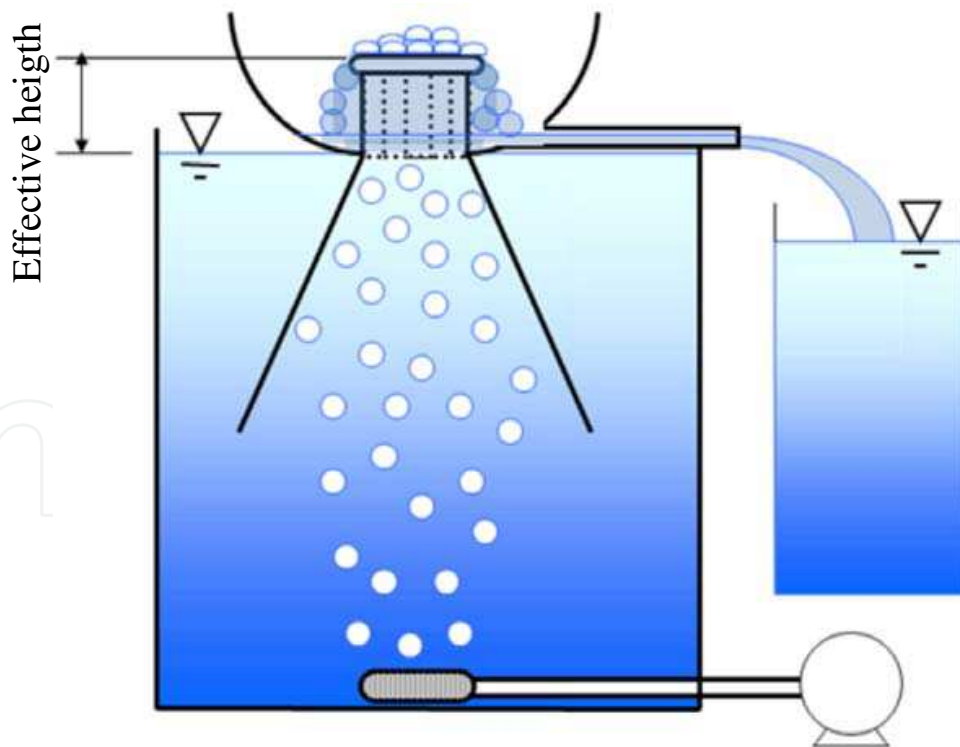


Fig. 19. Experimental apparatus relating to various effective heights

4.5.2 Results and discussion

Fig. 20 shows the effect of effective height on DO saturation rate, liquid/gas ratio and E_0 .

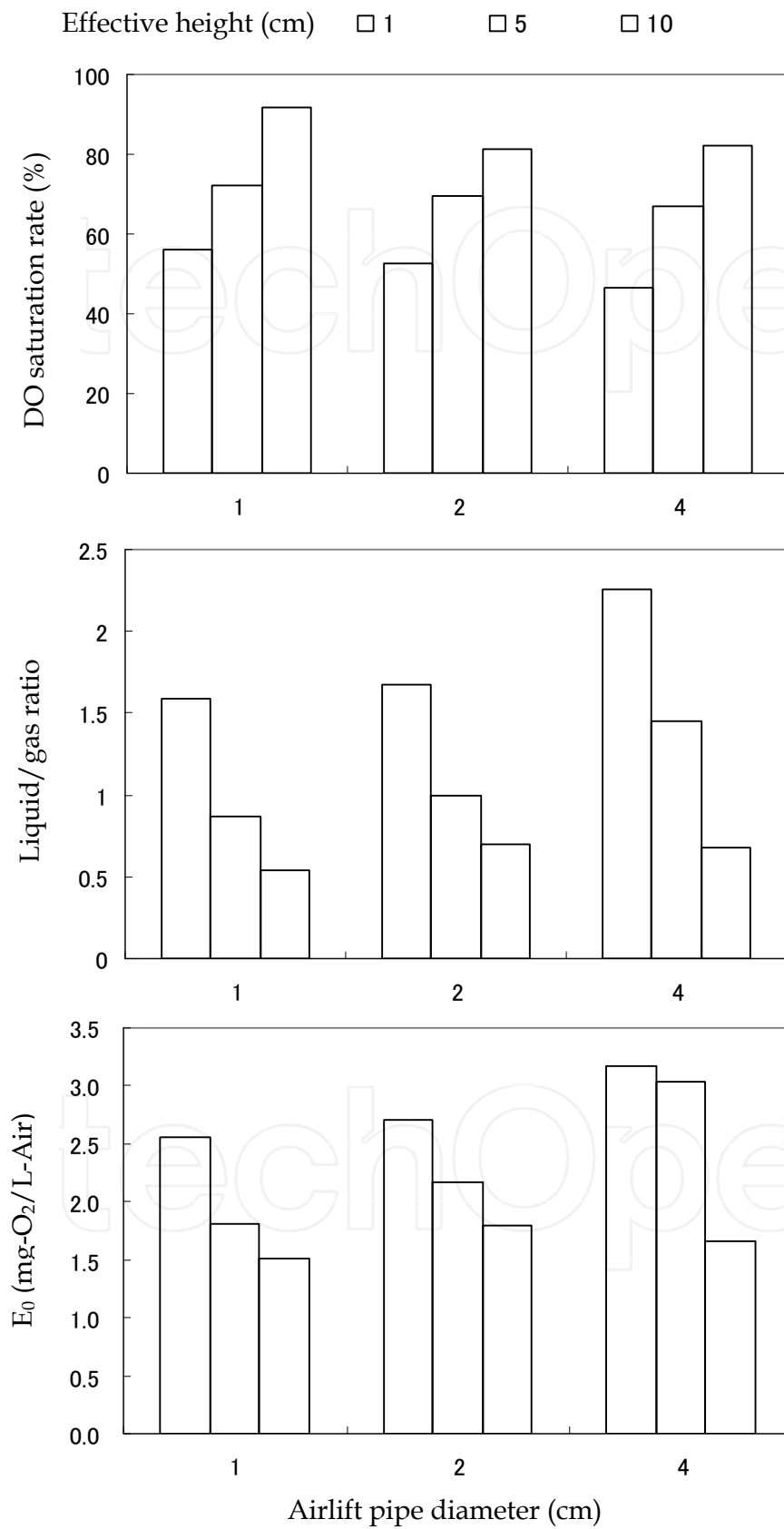


Fig. 20. Experimental findings as a function of effective height

The effluent flow rate displays a decreasing trend with increasing effective height. This can be explained by the fact that the higher the effective height in the atmosphere is, the larger the hydraulic head loss and the weaker the airlift effect are. DO saturation rate shows a propensity of going up of an increase in effective height. It can be easily understood that increased effective height leads to the prolonged contact time between the effluent water and air. Furthermore, in the case where the amount of the effluent water through the airlift pipes is reduced, a thinner liquid film can be formed, which can enhance the oxygen dissolution efficiency.

As a result, the oxygen transfer amount per unit air aeration volume approaches its maximum value under the experimental conditions of 1 and 5 cm in effective height, and 4 cm in pipe diameter.

4.6 Effect of the distribution of airlift pipes on oxygen supply efficiency

4.6.1 Experimental conditions and methods

Using highly oxygen-transfer-efficient airlift part with a pipe diameter of 4 cm and effective height of 1 cm, as shown in Fig. 21, we examine the effect of airlift part configuration by arranging 1, 2 and 3 pipes inside. To keep aeration flux constant, air flow rate normalized to each piece of airlift pipe is set at 6 L/min. The detailed experimental conditions are tabulated in Table 5.

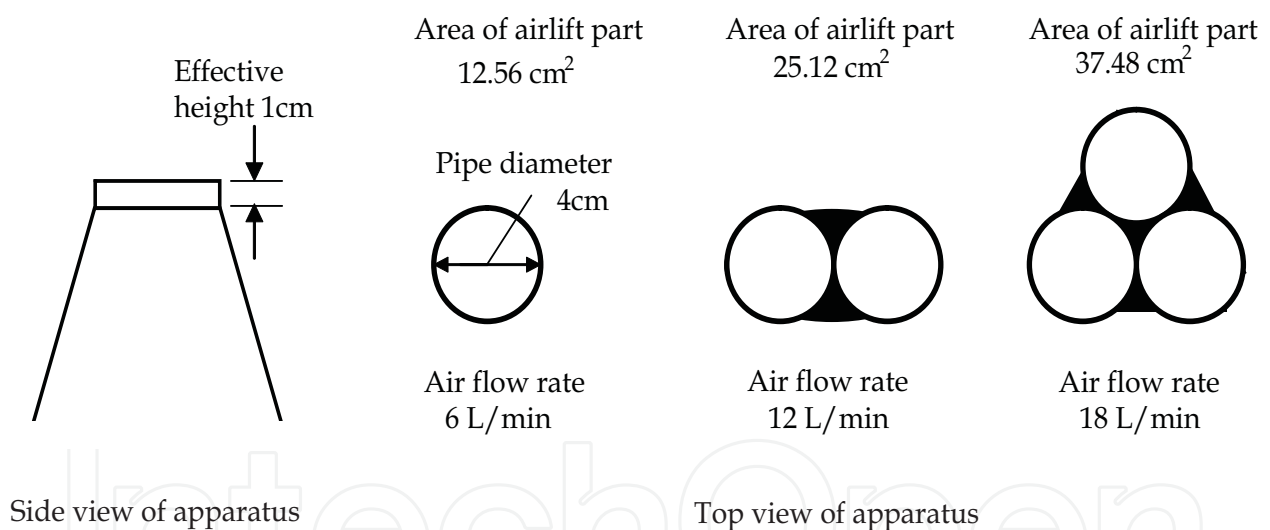


Fig. 21. The configuration of airlift part

Pipe diameter (cm)	Effective height (cm)	No. of airlift pipe	Cross-sectional area (cm ²)	Air flow rate per unit airlift pipe number (L/min)
4	1	1	12.56	6
		2	25.12	12
		3	37.48	18

Table 5. Experimental conditions relating to the configuration of the airlift part

4.6.2 Results and discussion

Figs. 22, 23, 24 and 25 respectively illustrate the effect of No. of airlift pipe on the effluent water flow rate per unit airlift pipe number, DO saturation rate in the effluent water, oxygen mass flow rate per unit airlift pipe number and oxygen transfer amount per unit cross-sectional area (cm^2) of airlift part.

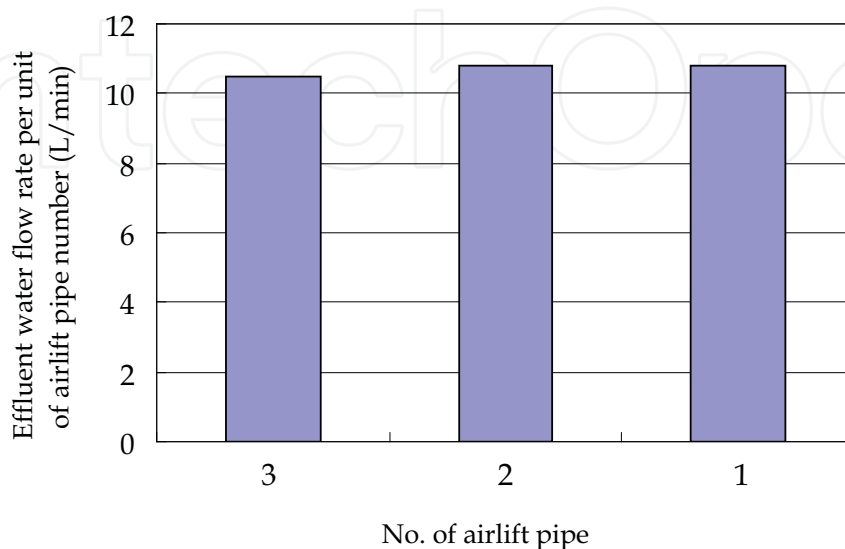


Fig. 22. Effect of airlift pipe No. on the effluent water flow rate per unit airlift pipe number

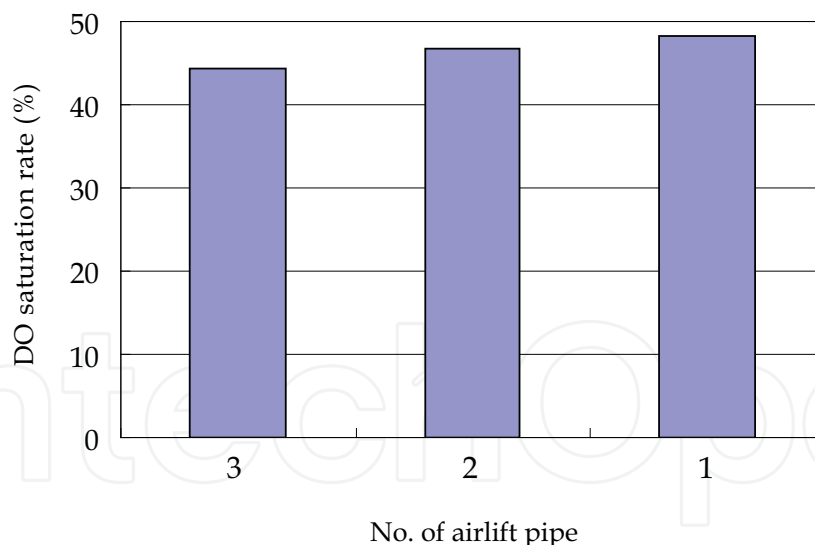


Fig. 23. Effect of airlift pipe No. on the DO saturation rate

As shown in Fig. 23, the lower the airlift pipe number is, the higher the DO saturation rate is. As revealed in Fig. 22, the effluent water flow rate per unit airlift pipe number does not change notably. Thus it appears that the aeration is evenly distributed among the airlift pipes. Namely, the air flow rate is the same through every airlift pipe. As revealed in Figs. 24 and 25, respectively, the oxygen transfer amount per unit airlift pipe number and oxygen transfer amount per unit airlift part cross-sectional area both exhibit a decreasing trend with increasing pieces of airlift pipes. If the air flow rate of every airlift pipe was same

(6 L/min), the same result is supposed to be obtained. On the contrary, the experimental data from Figs. 24 and 25 both tend to decay. This is due to the fact that for 1 piece of airlift pipe, the effluent can completely overflow through the periphery of the pipe. However, for 2 or 3 pieces of airlift pipes, a fraction of effluent overflowing from a certain airlift pipe can flow back into another airlift pipe, or 2 streams of effluents overflowing from 2 airlift pipes can hinder with each other, and thus flow back into the respective airlift pipes again, thereby causing the reduced effluent flow rate. Otherwise, with increasing airlift pipe number, the coverage area of the capture part is also increased. However, since only one diffuser is serving, it is impossible for aeration to uniformly distribute towards every airlift pipe. As a consequence, when designing the system, every airlift pipe should be separately installed. In the meanwhile, the design of the capture part should take into consideration that the gas bubbles can be well captured, and subsequently uniformly distributed to every airlift pipe.

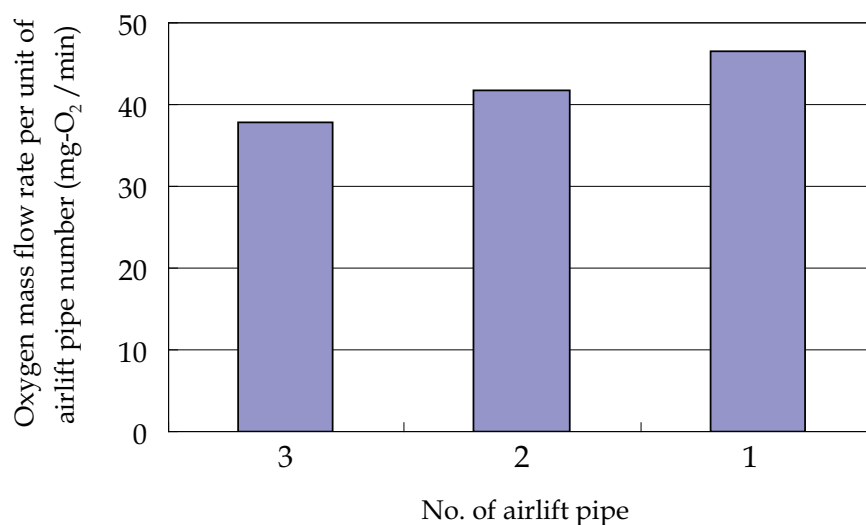


Fig. 24. Effect of airlift pipe No. on the oxygen mass flow rate per unit airlift pipe number

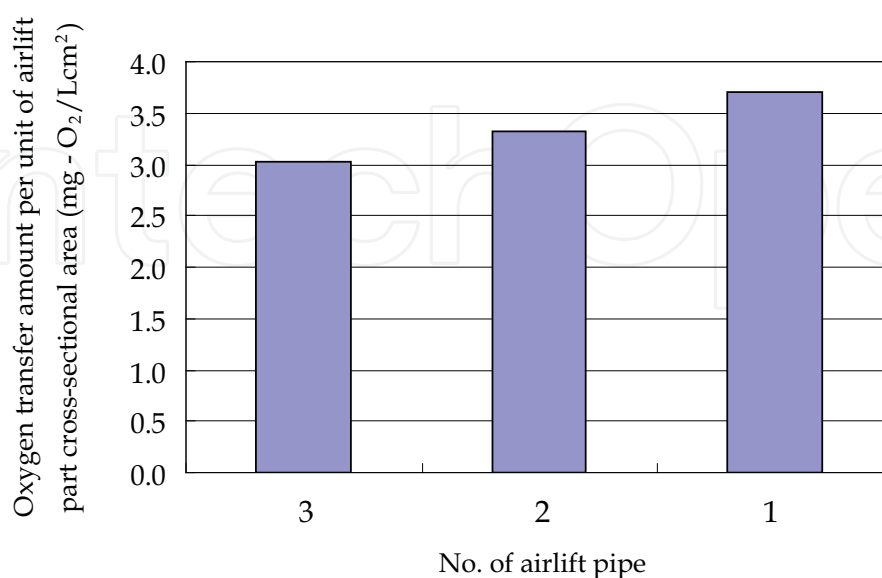


Fig. 25. Effect of airlift pipe No. on the oxygen transfer amount per unit airlift part cross-sectional area (cm²)

4.7 Effect of air flow rate on oxygen supply efficiency

4.7.1 Experimental conditions and methods

At a cross-sectional area of 12.56 cm², the impact of air flow rate on oxygen supply efficiency is studied experimentally. The experimental conditions include the air flow rate ranging from 6 to 18 L/min with an increment of 2 L/min. The pipe diameter of 4 cm and effective height of 1 cm are chosen for the LFFA. The experimental conditions in detail are presented in Table 6.

Pipe diameter (cm)	Effective height (cm)	Cross-sectional area (cm ²)	Air flow rate (L/min)
4	1	12.56	6, 8, 10, 12, 14, 16, 18

Table 6. Experimental conditions focusing on the variation in air flow rate

4.7.2 Results and discussion

Figs. 26, 27 and 28 respectively present the effects of air flow rate on the liquid/gas ratio, DO saturation rate and oxygen transfer amount normalized to 1 L of air (E_0).

As indicated in Fig. 26, at all air flow rates except for that of 6 L/min, any liquid/gas ratio does not change too much. It is thus deduced that the energy loss is very low in the airlift part. The findings of DO saturation rate are shown in Fig. 27. Below 12 L/min, it does not make a difference. In contrast, beyond 14 L/min, DO saturation rate exhibits an attenuating tendency. Thus, the excess air flow rate brings about the energy waste. As revealed in Fig. 28, oxygen transfer amount normalized to 1 L of aeration air is gradually increasing in the 6-12 L/min range. However, below 14 L/min, it tends to decrease gradually. Owing to nearly unchanged liquid/gas ratio shown in Fig. 26, the dominant factor affecting oxygen transfer rate is DO concentration. The reason lies in that with air flow rate increasing, it will lead to increasing effluent flow rate, rendering too much effluent water flowing through the airlift part in relation to gas bubble number, thereby inhibiting the liquid-film formation. In summary, under the present experimental conditions, the optimal air flow rate normalized to 1 cm² of cross-sectional area is 1.1 L/min.

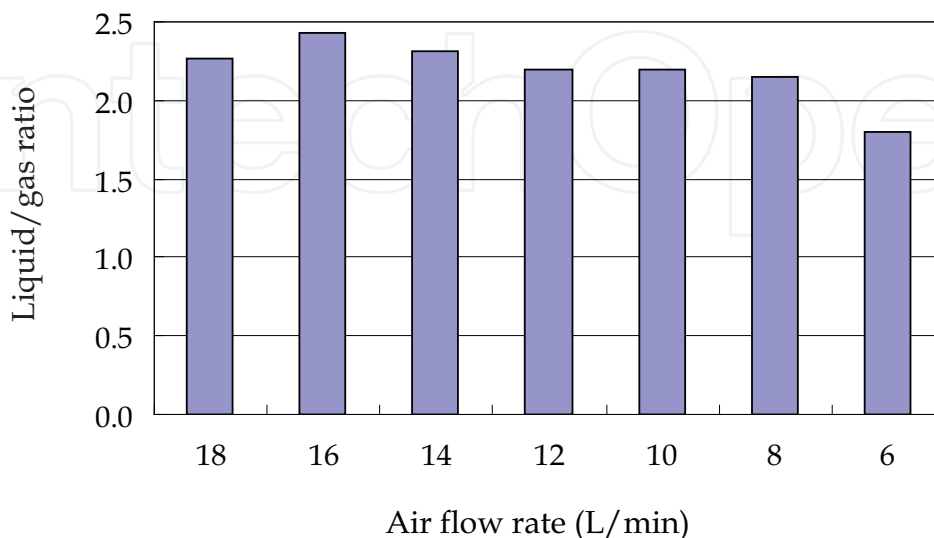


Fig. 26. Effect of air flow rate on the liquid/gas ratio

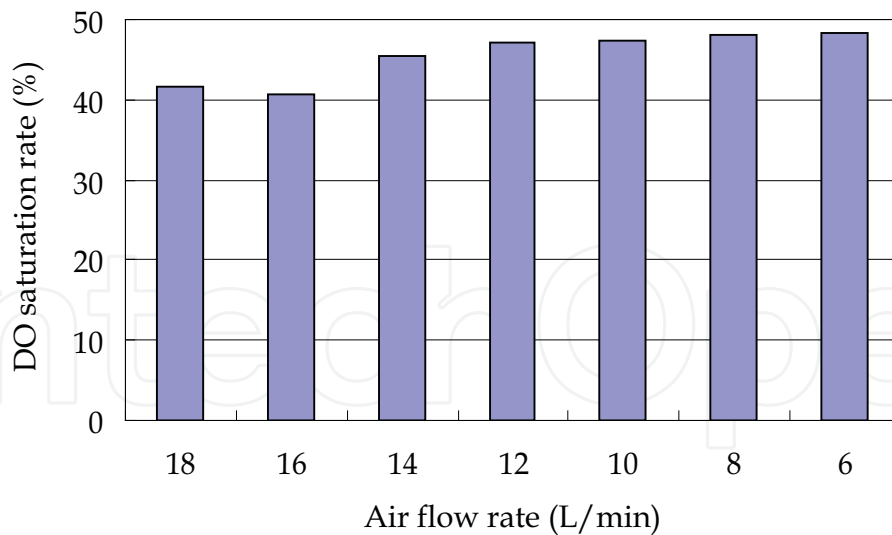


Fig. 27. DO saturation rate as a function of air flow rate

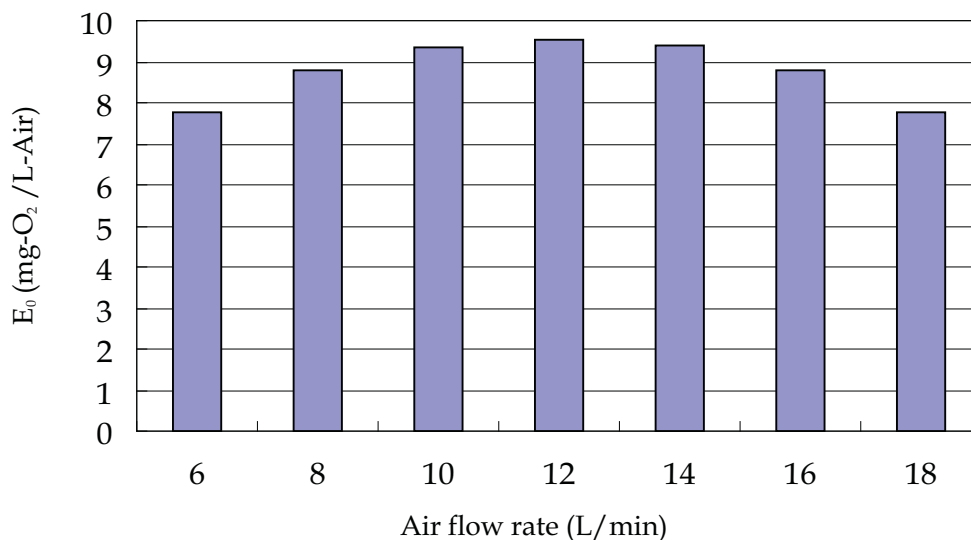


Fig. 28. E_0 as a function of air flow rate

5. Comparison of liquid film and conventional aeration systems in regard to k_La

5.1 Introduction

The performance of aeration apparatus is compared in terms of the k_La values of the liquid film and conventional aeration systems. Meanwhile, the effectiveness of LFFA is corroborated by calculating an important energy-saving index-oxygen transfer efficiency E_A , which is defined as the ratio of DO content to aeration-supplying oxygen amount.

5.2 Experimental conditions and methods

By means of a recycling liquid-film apparatus (4 cm in each individual airlift pipe diameter, 1 cm in effective height, 12.56 cm² in cross-sectional area of the airlift part), liquid film aeration tests in a 53 cm deep, 80 L water tank with a surface area of 1510 cm² are carried out

by applying air flow rates of 6, 8, 12 and 12.8 L/min. As a control, under the otherwise identical experimental conditions, the conventional aeration test is also investigated in this study. The experimental apparatus is shown in Fig. 29.

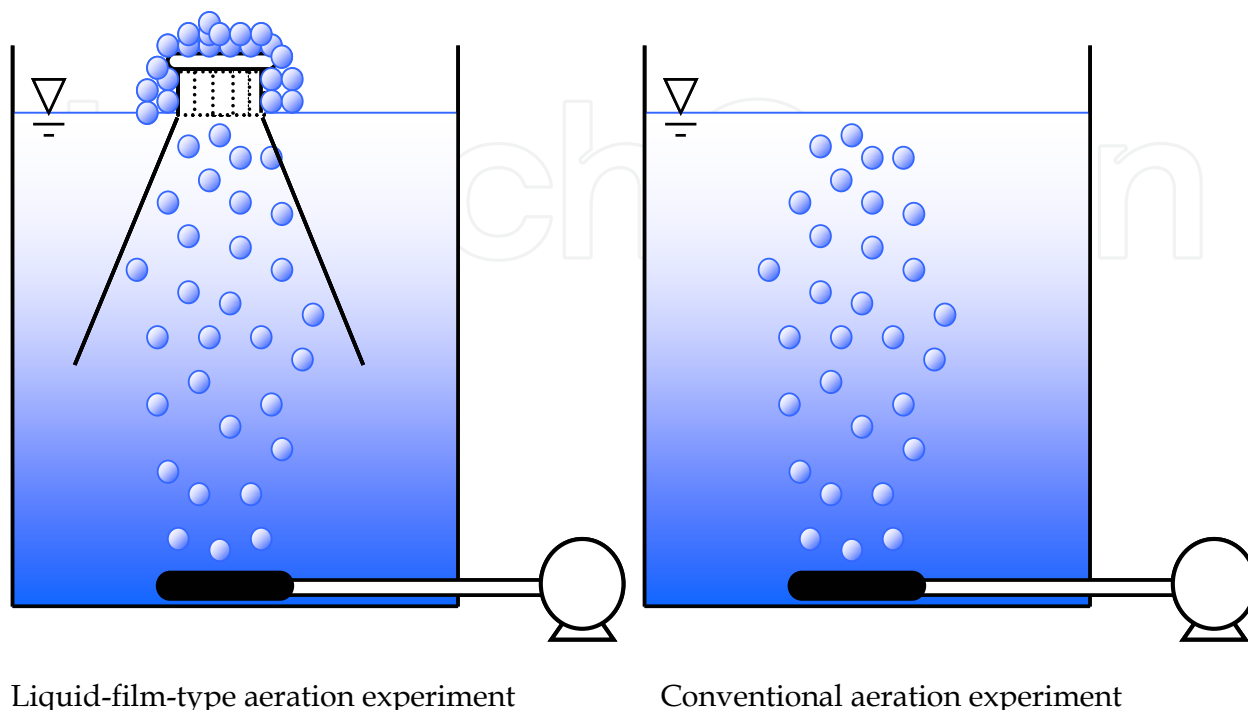


Fig. 29. The experimental apparatus diagrams of liquid-film aeration system and conventional aeration system

5.3 Calculation methods

The calculation method for total volumetric mass transfer coefficient (k_{LA}) follows the ASCE Standard for Measurement of Oxygen Transfer in Clean Water [18]. Then the obtained k_{LA} is calibrated to a standard reference temperature of 20 °C by using Equation (5) [16, 18],

$$k_{LA}(20) = 1/\gamma \times k_{LA}(T) \times 1.024^{(20-T)} \tag{5}$$

where $k_{LA}(20)$ and $k_{LA}(T)$ (hr^{-1}) are k_{LA} at 20 °C and the actual water temperature of T °C, respectively, γ is the activity coefficient of salt concentration and $\gamma = 8.8 \times 10^{-6} \times C_z + 1$, C_z (mg l^{-1}) represents the concentration of sodium sulfite solution.

The performance of oxygen mass transfer is assessed in terms of oxygen mass transfer efficiency, which is calculated based upon Equation (6) [19],

$$E_A(20) = \frac{DO_S(20) \cdot k_{LA}(20) \cdot V \times 10^{-3}}{G_S(20) \cdot \rho \cdot O_w} \times 100 \tag{6}$$

where $E_A(20)$ refers to oxygen transfer efficiency at 20 °C, $k_{LA}(20)$ ($1/\text{hr}$) is k_{LA} at 20 °C, $DO_S(20)$ (mg/L) is liquid-phase saturated DO concentration at 20 °C, $G_S(20)$ (m^3/hr) is air flow rate at 20 °C and 1 atm, V (m^3) is effective capacity of water tank, ρ is air density at 20°C and 1 atm ($\rho = 1.204 \text{ kg/m}^3$), and O_w (-) is oxygen content in air ($O_w = 0.233 \text{ O}_2\text{-kg/air-kg}$).

5.4 Results and discussion

As shown in Table 7 and Fig. 30, $k_L a(20)$ of liquid film aeration system displays an evolving trend same as that of conventional aeration system. That is, in the air flow rate range of 6-12 L/min, it gradually increases with increasing air flow rate. Beyond the upper limit, it will decrease slowly. However, as shown in Table 7 and Fig. 31. The $E_A(20)$ values of both liquid film aeration system and conventional aeration system decrease with increasing air flow rate.

Air flow rate(L/min)	$k_L a(20)$ (1/hr)		$E_A(20)$ (%)	
	Liquid film aeration system	Conventional aeration system	Liquid film aeration system	Conventional aeration system
6	9.6	8.4	6.64	5.81
8	12.4	11.2	6.39	5.78
12	14.9	14.0	5.12	4.81
12.8	12.2	13.2	4.02	4.33

Table 7. Comparison of liquid film aeration system with conventional aeration system

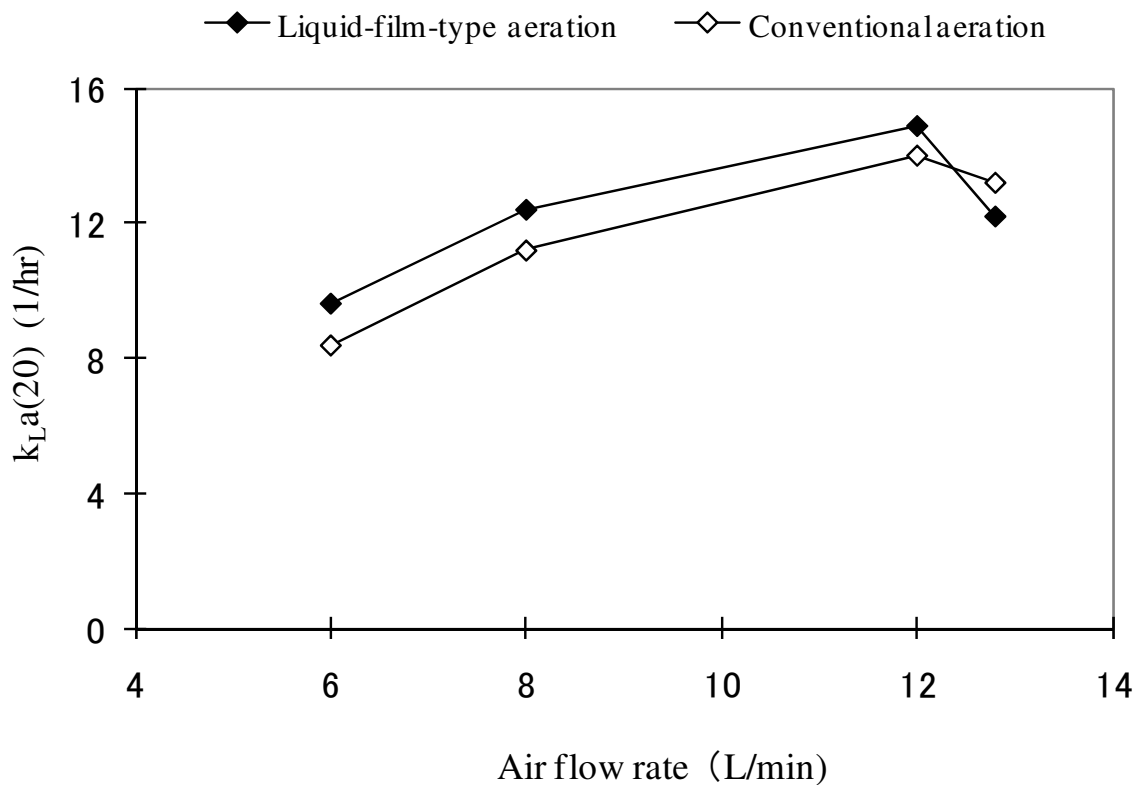


Fig. 30. The comparative data of $k_L a(20)$ of liquid film and conventional aeration systems

As compared with $k_L a(20)$ and $E_A(20)$ of both aeration systems, at the air flow rate ranging from 6 to 12 L/min, the aeration efficiency of liquid film aeration system increases by 6.3-14.3%. Particularly at the air flow rate of 6 L/min, $E_A(20)$ is still up to 6.64% even utilizing a very shallow aeration depth of 0.5 m. The efficiency of liquid-film aeration is enhanced by 14.3% relative to the conventional aeration system under the identical conditions.

As indicated above, water body can form a liquid film in the atmosphere. The LFFA can remarkably improve oxygen supply efficiency by simultaneously contacting the interior and exterior of the resulting liquid film with the air.

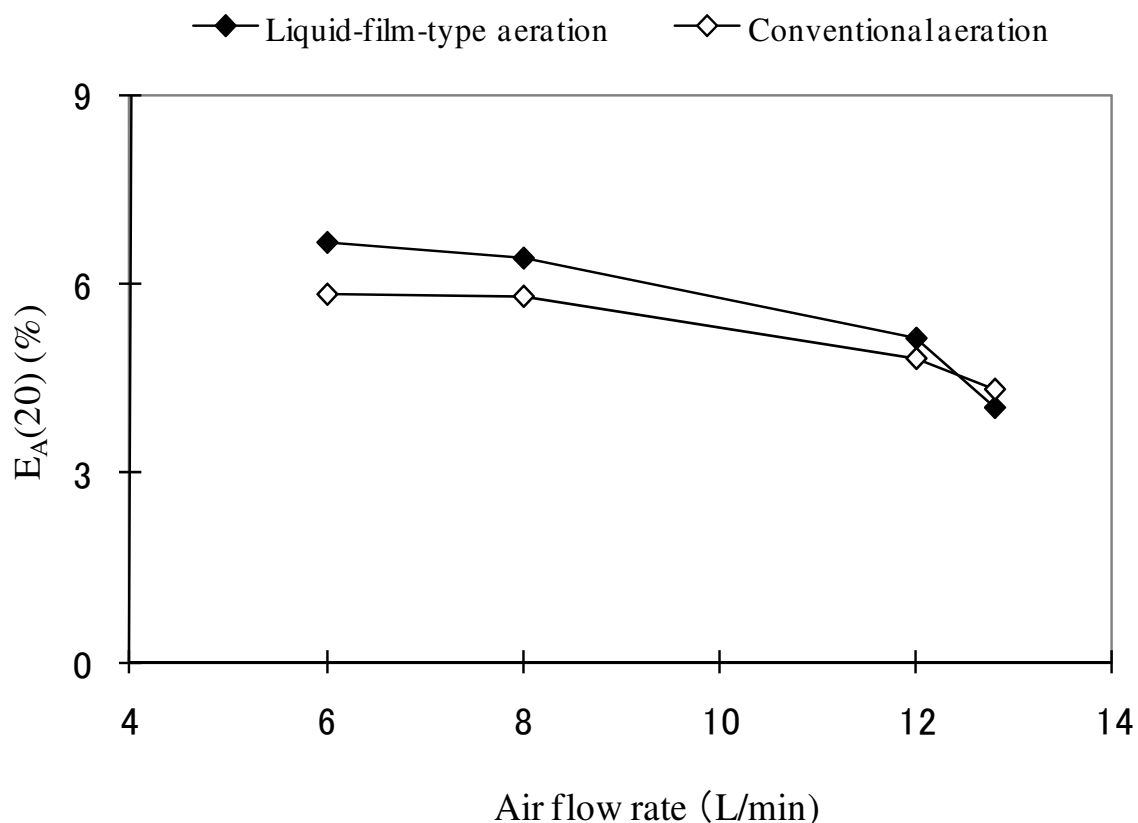


Fig. 31. The comparison data of $E_A(20)$ of liquid film and conventional aeration systems

6. Analysis of the performance of LFFA

6.1 Introduction

In order to evaluate the oxygen transfer performance of the LFFA, in this section, the overall oxygen transfer process is divided into two-step oxygen transfer. That is, in the conventional aeration system, oxygen transport process is split into bubble transfer and surface transfer. In contrast, in the liquid film aeration system, it is divided into bubble transfer and liquid film transfer. Oxygen transfer efficiency of every step is separately derived from the experiment. The performance of the LFFA is thus evaluated.

6.2 Experimental conditions and methods

By means of a recycling liquid film apparatus (4 cm in each individual airlift pipe diameter, 1 cm in effective height, 12.56 cm² in cross-sectional area of the airlift part), liquid film aeration tests in a 53 cm deep, 80 L water tank with a surface area of 1510 cm² are carried out applying an air flow rate of 6 L/min. As a control, under the otherwise identical experimental conditions, the conventional aeration test with air and diffused test with nitrogen are both investigated in this study. Their experimental apparatuses are shown in Fig. 32.

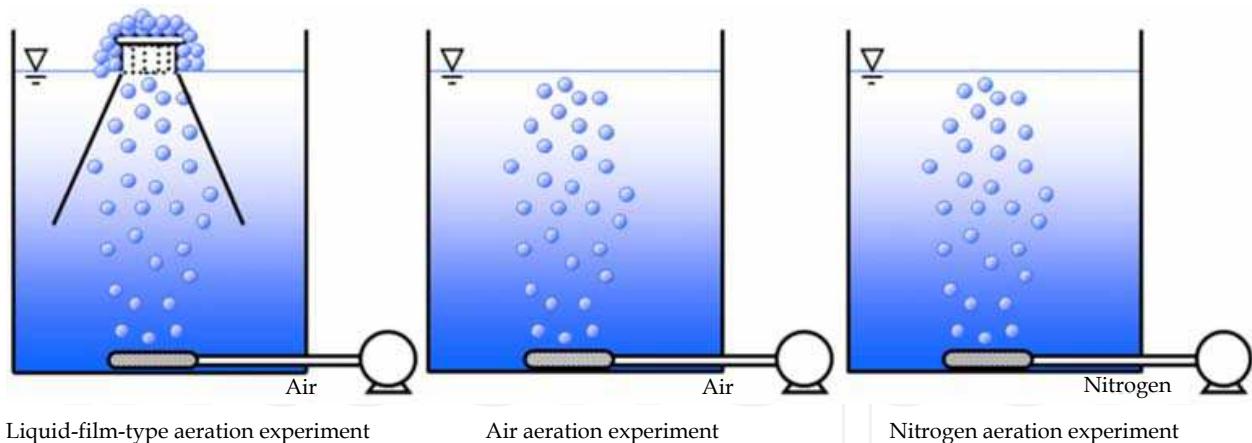


Fig. 32. Experimental apparatuses of testing liquid film aeration with air, and conventional aerations with air and nitrogen, respectively

6.3 Calculation methods

The calculation method for total volumetric mass transfer coefficient ($k_{L}a$) follows the ASCE Standard for Measurement of Oxygen Transfer in Clean Water [18]. Then the obtained $k_{L}a$ is calibrated to a standard reference temperature of 20 °C by using Equation (5) [16, 18].

When a submerged diffuser is operating, there are two main interfaces through which oxygen transfer occurs, *i.e.*, bubble-water interface and air-water interface, as reflected in Equation (7) [2, 3],

$$\frac{dC}{dt} = \frac{k_{L}a_b}{h_d} \int_z (C_o^* - C) dz + k_{L}a_s (C_{sat} - C) \quad (7)$$

where $k_{L}a_b$ (1/hr) is the volumetric mass transfer coefficient for bubble surface, $k_{L}a_s$ (1/hr) is the volumetric mass transfer coefficient for water surface, h_d (m) is the depth from diffuser to water surface, z (m) is a variable distance from the diffuser, C_{sat} (mg/L) is the saturation oxygen concentration in water at atmospheric pressure, C (mg/L) is the actual DO concentration in water body and C_o^* (mg/L) is the liquid-phase equilibrium oxygen concentration of a bubble. C_o^* is not only a function of temperature and atmospheric pressure, but also hydrostatic pressure and gas-phase oxygen composition. Over depth, the bubble transfer of all gases affects the gas-phase oxygen composition and the equilibrium oxygen concentration.

Wilhelms and Martin developed an approach to split surface and bubble transfer by releasing nitrogen gas from a diffuser rather than air [1]. Herein, it is assumed that no oxygen is initially present in the bubbles, thereby eliminating the estimation of a value for concentration inside the bubbles. Additionally, as a result of utilizing the complete and shallow-depth aeration approach in this set of experiments, the contribution of water depth to DO concentration distribution is thus negligible. That is because the DO concentration is considered to be approximately constant over space in the whole water tank. Under such assumptions, Equation (7) can be rewritten as Equation (8),

$$\frac{dC}{dt} = k_{L}a_b(0 - C) + k_{L}a_s(C_{sat} - C) \quad (8)$$

Steady state is reached between the absorption of oxygen through surface transfer and the stripping of oxygen from the water by nitrogen bubbles, *i.e.*, $dC/dt = 0$. The formula can be hence deduced as follow,

$$\frac{k_L a_b}{k_L a_s} = \frac{C_{sat} - C_n}{C_n} \quad (9)$$

where C_n (mg/L) is the steady-state DO concentration in the diffused tests with nitrogen. $k_L a_b$ and $k_L a_s$ are calculated based upon Equation (9).

6.4 Results and discussion

DO concentration versus time curves for liquid film and conventional aeration tests as well as diffused test with nitrogen are illustrated in Fig. 33. The ultimate steady-state DO concentrations are 8.39 mg/L for the conventional aeration trial, 8.72 mg/L for the liquid film aeration trial and 0.94 mg/L for the diffused test with nitrogen.

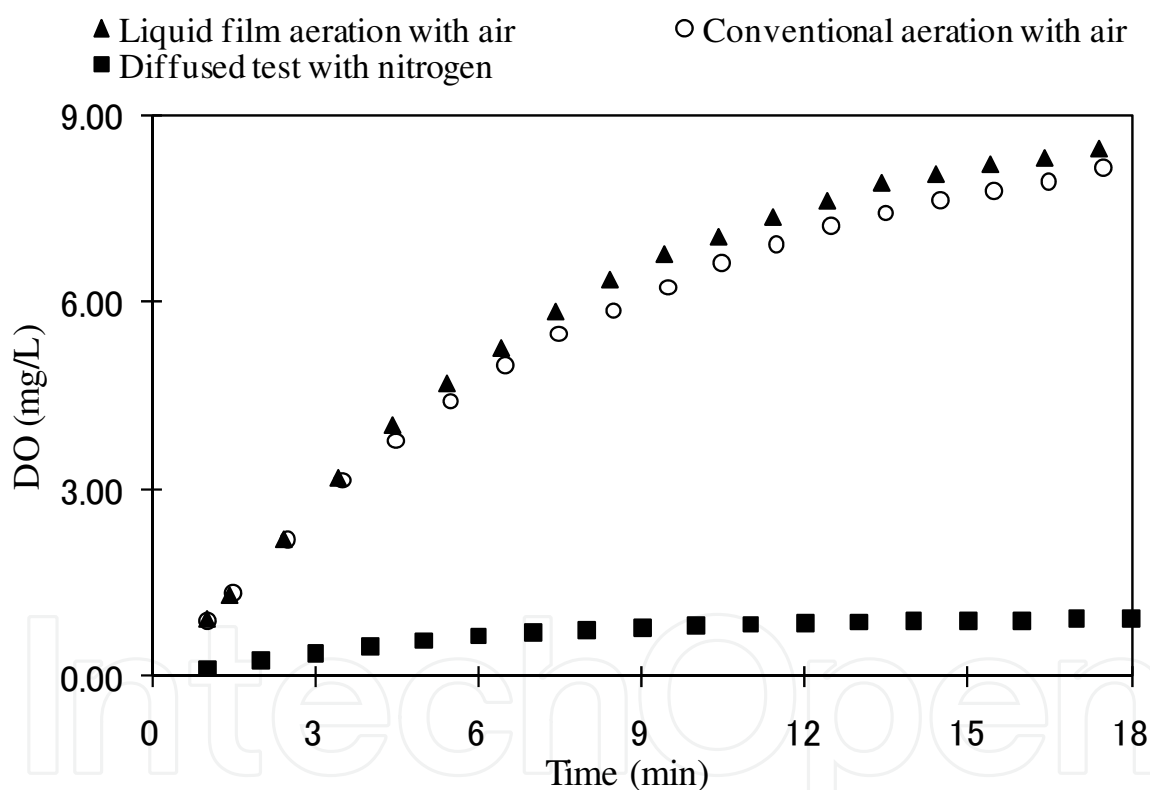


Fig. 33. DO concentration vs. time curves for liquid film aeration and conventional aeration tests as well as diffused test with nitrogen ($C_{sat} = 8.84$ mg/L)

Table 8 presents the calculation data derived from the experimental results shown in Fig. 33. Under the operating conditions of 80 L in water capacity, 53 cm in aeration depth, 1510 cm² in surface area and 6 L/min in air flow rate, a $k_L a(20)$ value of 8.4 hr⁻¹ for the conventional aeration system is calculated. In contrast, the level of $k_L a(20)$ for the liquid film aeration system with the relevant LFFA installed simply on the water surface is 9.6 hr⁻¹ (*cf.* Table 8). As compared with these data, the $k_L a(20)$ is increased by about 14% as a consequence of the substantial oxygen transfer contribution from the LFFA.

The $k_L a_b$ and $k_L a_s$ of conventional aeration testings are shown in Table 8 (i.e., $k_L a_b = 7.5 \text{ hr}^{-1}$ and $k_L a_s = 0.9 \text{ hr}^{-1}$). That is, in a water tank with a water loading of 80 L, aeration depth of 53 cm, and surface area of 1510 cm², while aerating at an air flow rate of 6 L/min, oxygen transfer amount through water surface has a share of roughly 11% of the overall oxygen transfer quantity.

The oxygen transfer of liquid film aeration involves oxygen transfers through gas bubbles, water surface and liquid film. Because the experimental conditions such as aeration depth, aeration amount and gas bubble diameter are identical between the conventional aeration and liquid film aeration, it is reasonable to consider that gas bubble based oxygen transfer capabilities are same in both cases. For the water surface based oxygen transfer ability, liquid film aeration apparatus only occupies a water surface area of 12.56 cm² out of the total surface area of 1510 cm², taking up roughly 0.83% of the whole water surface area. Hence, the coverage area from the liquid film apparatus is completely negligible. However, because the disturbance effect of the liquid film apparatus on the water surface can not be estimated (either positive or negative action), in this discussion, water surface based oxygen transfer capacity is hard to be regarded as same in both cases. Accordingly, the liquid film based oxygen transfer capacity can not be accurately quantified. For the liquid-film aeration experiment, the oxygen transfers through the water surface and liquid film are thus summed up as an overall entity.

Based upon the reason above, the $k_L a_b$ and $k_L a_s$ of a liquid-film aeration system are derived as 7.5 and 2.1 hr⁻¹, respectively. Namely, the oxygen transfer amount via water surface accounts for 22% of overall oxygen transfer capacity.

As shown in Table 8, water surface based oxygen transfer efficiency by means of liquid film aeration apparatus is enhanced to 2.3 times in relation to that by the conventional aeration setup.

$k_L a$ (hr ⁻¹)	Conventional aeration system	Liquid-film aeration system
$k_L a_t$	8.4	9.6
$k_L a_b$	7.5	7.5
$k_L a_s$	0.9	2.1

$k_L a_t$: total volumetric mass transfer coefficient.

$k_L a_b$: volumetric mass transfer coefficient for bubble surface.

$k_L a_s$: volumetric mass transfer coefficient for water surface.

Table 8. Comparative results for $k_L a$ between the conventional aeration and liquid-film aeration systems.

7. Summary

Through a series of experiments, it is proven that the oxygen transfer rate of liquid-film aeration system is higher than that of conventional aeration system. Furthermore, the former can transiently produce the water with a high DO concentration. Obviously, this efficient aeration process is considered as a less energy-intensive alternative to current aeration methods.

By exploring a range of design factors affecting oxygen transfer efficiency of the LFFA, various design parameters of the LFFA are basically determined. The optimal structural parameters of the LFFA are identified to be 4 cm in airlift pipe diameter, ca. 1 cm in effective height and 1.1 L/min in air flow rate per unit cross-sectional area of an airlift part.

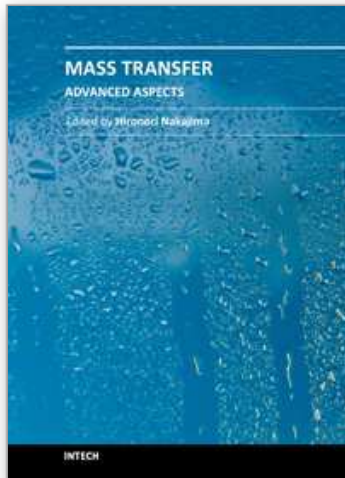
By forming a liquid film in the LFFA, the water surface based oxygen transfer efficiency increases by a factor of approximately 2.3 in comparison to the conventional aeration system. The overall oxygen transfer efficiency is raised to 14%. Especially, even at a very shallow aeration depth of 0.5 m, its $E_A(20)$ still reaches up to 6.64%. These data convincingly suggest that LFFA developed here has an effective oxygen transfer capacity. Meanwhile, as a result of forming a liquid film by LFFA, the effluent water of high DO concentration can be produced even at an aeration depth of about 0.5 m. Therefore, the conventional aeration depth can be reduced down to a very shallow extent by installing LFFA. A direct outcome is that the energy consumption from the air supply devices such as the blower is supposed to be greatly lowered, therefore saving the costs of both aeration-related equipment and operation.

8. References

- [1] Wilhelms, S. C. and Martin, S. K., Gas transfer in diffused bubble plumes, In Jennings S. M. and Bhowmilk N. G., Eds. *Hydraulic Engineering: saving a threatened resource-in search of solutions*. ASCE, New York, p.317-322, 1992.
- [2] McWhirter, J. R. and Hutter, J. C., Improved oxygen mass transfer modelling for diffused/subsurface aeration systems. *AIChE J.*, 35, p.1527-1534, 1989.
- [3] DeMoyer, C. D., Schierholz, L. E., Gulliver, J. S. and Wilhelms, S. C., Impact of bubble and free surface oxygen transfer on diffused aeration systems. *Water Res.*, 37, p.1890-1904, 2003.
- [4] Peterson, R. R., Design criteria for high purity oxygen treatment of kraft mill effluent. *J. Water Pollut. Control Fed.*, 47, p.2317-2329, 1975.
- [5] Nelson, J. K. and Puntenney, J. L., Performance comparison of the air and high purity oxygen activated sludge systems. *J. Water Pollut. Control Fed.*, 55, p.336-340, 1983.
- [6] Stenstrom, M. K., Kido, W., Shanks, R. F. and Mulkerin, M., Estimating oxygen transfer capacity of a full-scale pure oxygen activated sludge plant. *J. Water Pollut. Control Fed.*, 61, p.208-220, 1989.
- [7] Yuan, W., Okrent, D. and Stenstrom, M. K., Model calibration for the high-purity oxygen activated sludge process-algorithm development and evaluation. *Water Sci. Technol.*, 28, p.163-171, 1993.
- [8] Kuo, J. F., Dodd, K. M., Chen, C. L., Horvath, R. W. and Stahl, J. F. Evaluation of tertiary filtration and disinfection systems for upgrading high-purity oxygen-activated sludge plant effluent. *Water Environ. Res.*, 69, p.34-43, 1997.
- [9] Tzeng, C. J., Iranpour, R. and Stenstrom, M. K., Modelling and control of oxygen transfer in high purity oxygen activated sludge process. *J. Environ. Eng.-ASCE*, 129, p.402-411, 2003.
- [10] Jang, A. and Kim, I. S., Effect of high oxygen concentrations on nitrification and performance of high-purity oxygen A/O bio-film process. *Environ. Eng. Sci.*, 21, p.273-281, 2004.
- [11] Moore, T. L., Basic criteria and design aspects for deep aeration tanks. *Water Res.*, 6, p.407-412, 1972.

- [12] Polprasert, C. and Raghunandana, H. S., Wastewater treatment in a deep aeration tank. *Water Res.*, 19, p.257-264, 1985.
- [13] Gnirss, R. and Peter-Frölich, A., Biological treatment of municipal wastewater with deep tanks and flotation for secondary clarification. *Water Sci. Technol.*, 34, p.257-265, 1991.
- [14] Asselin, C., Comeau, Y. and Ton-That, Q. A., Alpha correction factors for static aerators and fine bubble diffusers used in municipal facultative aerated lagoons. *Water Sci. Technol.*, 38, p.79-85, 1998.
- [15] Gillot, S. and Héduit, A., Effect of air flow rate on oxygen transfer in an oxidation ditch equipped with fine bubble diffusers and slow speed mixers. *Water Res.*, 34, p.1756-1762, 2000.
- [16] Omatsu, R., Energy-saving efficiency of fine bubble diffuser in actual operation. *Kurimoto Research*, 48, p.2-7, 2003. (In Japanese).
- [17] Gillot, S., Capela-Marsal, S., Roustan, M. and Héduit, A., Predicting oxygen transfer of fine bubble diffused aeration systems-model issued from dimensional analysis. *Water Res.*, 39, p.1379-1387, 2005.
- [18] ASCE, Standard for the measurement of oxygen transfer in clean water, 2nd ed. ASCE, New York, 1993.
- [19] Sewerage Facilities Planning and Design Manual (Volume 2), Japan Sewage Works Association, Tokyo, 1994. (Japanese)

IntechOpen



Mass Transfer - Advanced Aspects

Edited by Dr. Hironori Nakajima

ISBN 978-953-307-636-2

Hard cover, 824 pages

Publisher InTech

Published online 07, July, 2011

Published in print edition July, 2011

Our knowledge of mass transfer processes has been extended and applied to various fields of science and engineering including industrial and manufacturing processes in recent years. Since mass transfer is a primordial phenomenon, it plays a key role in the scientific researches and fields of mechanical, energy, environmental, materials, bio, and chemical engineering. In this book, energetic authors provide present advances in scientific findings and technologies, and develop new theoretical models concerning mass transfer. This book brings valuable references for researchers and engineers working in the variety of mass transfer sciences and related fields. Since the constitutive topics cover the advances in broad research areas, the topics will be mutually stimulus and informative to the researchers and engineers in different areas.

How to reference

In order to correctly reference this scholarly work, feel free to copy and paste the following:

Tsuyoshi Imai and Hua Zhu (2011). Improvement of Oxygen Transfer Efficiency in Diffused Aeration Systems Using Liquid-Film-Forming Apparatus, *Mass Transfer - Advanced Aspects*, Dr. Hironori Nakajima (Ed.), ISBN: 978-953-307-636-2, InTech, Available from: <http://www.intechopen.com/books/mass-transfer-advanced-aspects/improvement-of-oxygen-transfer-efficiency-in-diffused-aeration-systems-using-liquid-film-forming-app>

INTECH
open science | open minds

InTech Europe

University Campus STeP Ri
Slavka Krautzeka 83/A
51000 Rijeka, Croatia
Phone: +385 (51) 770 447
Fax: +385 (51) 686 166
www.intechopen.com

InTech China

Unit 405, Office Block, Hotel Equatorial Shanghai
No.65, Yan An Road (West), Shanghai, 200040, China
中国上海市延安西路65号上海国际贵都大饭店办公楼405单元
Phone: +86-21-62489820
Fax: +86-21-62489821

© 2011 The Author(s). Licensee IntechOpen. This is an open access article distributed under the terms of the [Creative Commons Attribution 3.0 License](#), which permits unrestricted use, distribution, and reproduction in any medium, provided the original work is properly cited.

IntechOpen

IntechOpen